

AD-771 188

TUNABLE OPTICAL SOURCES

S. E. Harris, et al

Stanford University

Prepared for:

Army Research Office-Durham  
Advanced Research Projects Agency

September 1973

DISTRIBUTED BY:

**NTIS**

National Technical Information Service  
U. S. DEPARTMENT OF COMMERCE  
5285 Port Royal Road, Springfield Va. 22151

ARO: 7580.17. (1) FG  
(1)

# **TUNABLE OPTICAL SOURCES**

## **Semiannual Report**

for

U. S. Army Research Office (Durham)

Contract No. DA-ARO-D-31-124-72-G-184

Sponsored by

Advanced Research Projects Agency

ARPA Order No. 675, Am 7

Program Code No. 9E20

for the period

1 April 1973 - 30 September 1973

M. L. Report No. 2217

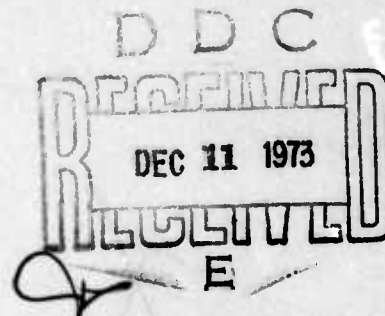
September 1973

Reproduced by  
**NATIONAL TECHNICAL  
INFORMATION SERVICE**  
U S Department of Commerce  
Springfield VA 22151

**Microwave Laboratory**  
**W. W. Hansen Laboratories of Physics**  
**Stanford University**  
**Stanford, California**

Approved for public release; distribution  
unlimited.

The findings in this report are not to be construed as an  
official Department of the Army position, unless so  
designated by other authorized documents.



99R

AD 771188

Scientific Personnel

on

U. S. Army Research Office (Durham)

Contract No. DA-ARO-D-31-124-72-G-184

1 April 1973 - 30 September 1973

S. E. Harris

Principal Investigator

R. L. Byer

Assistant Professor

J. F. Young

Research Associate

R. L. Herbst

Research Associate

D. M. Bloom

Research Assistant

M. M. Choy

Research Assistant

E. A. Stappaerts

Research Assistant

S. Warshaw

Research Assistant

Phone: (415) 327-7800

## I. RESEARCH OBJECTIVES

This grant supports research into new methods and techniques for the generation of tunable radiation across wide regions of the electromagnetic spectrum. During the past semiannual period progress in both vacuum ultraviolet and tunable infrared generation has been considerable. This report describes the work in both of the above research areas.

## II. TUNABLE INFRARED GENERATION

### A. Introduction

In the last report the infrared nonlinear properties of CdSe for mixing were described. Generation of wavelengths between  $9\mu$  and  $27\mu$  is possible in CdSe with good efficiency. One drawback to CdSe is inadequate birefringence for generation of infrared wavelengths shorter than  $9\mu$ . Fortunately, a chalcopyrite crystal,  $\text{AgGaSe}_2$ , has recently been grown which does have adequate birefringence to phasematch in the near infrared.

### B. $\text{AgGaSe}_2$

The properties of  $\text{AgGaSe}_2$  are described in a paper submitted for publication (see Appendix A). Mixing experiments to generate  $7\mu$  to  $15\mu$  have also been described in a paper presented at the first tunable laser spectroscopy conference at Vail, Colorado in July 1973. This paper is reproduced as Appendix B.

Briefly,  $\text{AgGaSe}_2$  has a high nonlinear coefficient, phasematches for mixing to generate between  $3\mu$  and  $18\mu$  radiation, and phasematches for SHG for fundamental wavelengths between  $3\mu$  and  $13\mu$ .  $\text{AgGaSe}_2$  is grown by the standard vertical Bridgeman method and low loss  $< 0.04 \text{ cm}^{-1}$  single crystals up to 15 mm in length have been obtained. These qualities make  $\text{AgGaSe}_2$  particularly attractive as a phasematchable infrared nonlinear crystal within its  $0.7\mu$  to  $18\mu$  transparency range.



$\text{AgGaSe}_2$  forms an ideal match to a  $\text{LiNbO}_3$  parametric oscillator source for generation of  $3\mu$  to  $18\mu$  radiation. A detailed study of a widely tunable coherent spectrometer based on a Nd:YAG pumped  $\text{LiNbO}_3$  parametric oscillator has been completed. The basic results of the study are given here.

### C. High Energy Widely Tunable Infrared Source

This section describes a unique combination of known methods and devices such that an extended  $0.3\mu - 27\mu$  and  $70\mu - 100\mu$  coherent tunable radiation source is possible. The device is based on a Nd:YAG laser pump source, a singly resonant  $\text{LiNbO}_3$  parametric oscillator and mixing in four nonlinear crystals,  $\text{AgGaSe}_2$ ,  $\text{CdSe}$ ,  $\text{LiNbO}_3$ , and  $\text{LiIO}_3$ . It is expected that the device will achieve continuous scanning at  $0.1 \text{ cm}^{-1}$  bandwidth at 10 mJ energy per pulse at 10 pps in the near infrared and visible and corresponding performance with the energy reduced by the Manley-Rowe factor in the intermediate and far infrared. Spectral bandwidths of the order of  $0.001 \text{ cm}^{-1}$  appears likely for narrow tuning ranges of approximately  $1 \text{ cm}^{-1}$ .

The features never before achieved that are unique to this source are:

1. 10 mJ energy per pulse
2. Wide infrared tuning range
3. Use of only 1 set of mirrors
4. Unique bandwidth control and local tuning methods
5. Rapid wide range tuning
6. Good frequency stability

The pump source is a Nd:YAG oscillator electro-optically Q-switched using a KD\*P pockels cell of standard design. The oscillator is operated TEM<sub>00</sub> mode and substantially single frequency by proper aperture and etalon control. Nd:YAG lasers meeting this requirement are presently in operation.

The Nd:YAG laser may be followed by a double pass Nd:YAG amplifier. The amplifier increases the Nd:YAG laser energy from 10 mJ to between 100 and 450 mJ depending on the filling factor of the amplifier rod. For this case the rod diameter is 6 mm and the length is 30 mm. Experimental verification of these results has been demonstrated.<sup>1</sup> If required, a further increase in energy output can be achieved with a second amplifier rod 1 cm in diameter and 30 mm in length. Figure 1 shows a schematic of the Nd:YAG pump source.

The LiNbO<sub>3</sub> parametric oscillator operates in the singly resonant mode with tuning achieved by crystal rotation.<sup>2</sup> Figure 2 illustrates the schematic of the oscillator including bandwidth control elements. Figure 3 shows the tuning curves versus crystal angle for a fixed temperature near 120°C.

The LiNbO<sub>3</sub> parametric oscillator is the key element in the chain of tuning elements that follow. Therefore, threshold, conversion, efficiency, tuning method, and bandwidth will be considered in detail.

The gain of the LiNbO<sub>3</sub> parametric oscillator is limited by the available laser pump energy or by the crystal damage threshold. We will investigate the gain limitations for off-angle phasematched operation, and compare it with 90° phasematched operation.

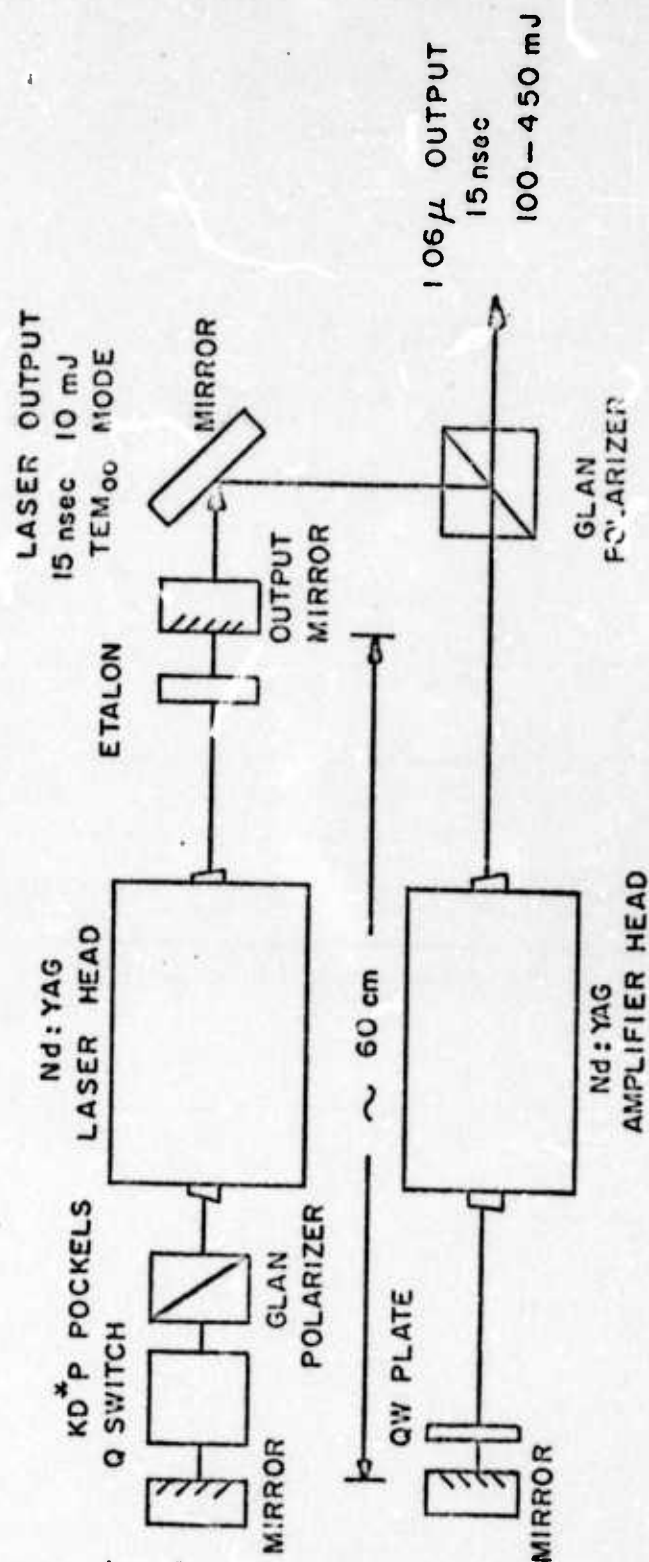


FIG. 1--Schematic of the 1.06 $\mu$  Nd:YAG laser-amplifier source.



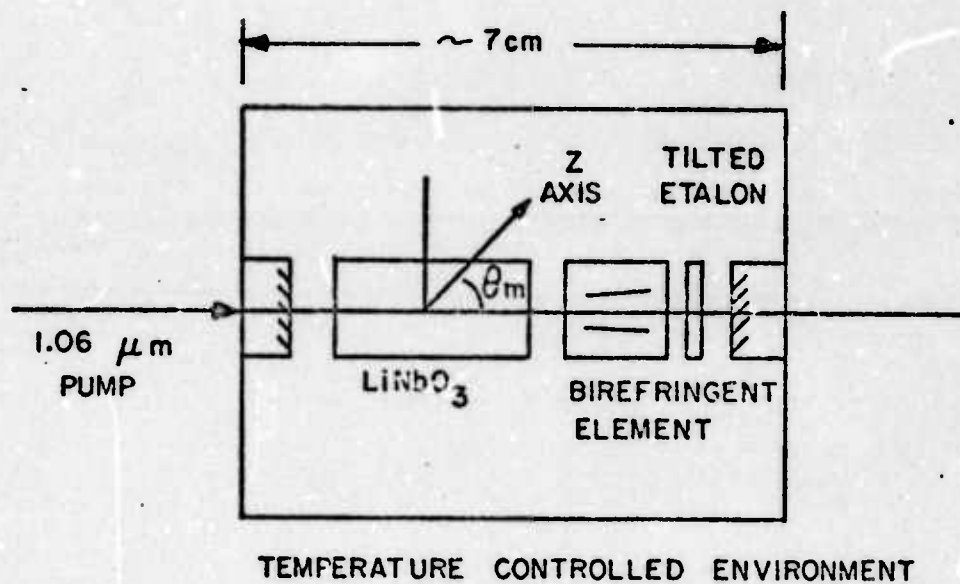


FIG. 2--Full scale schematic of the angle tuned  $\text{LiNbO}_3$  singly resonant parametric oscillator.

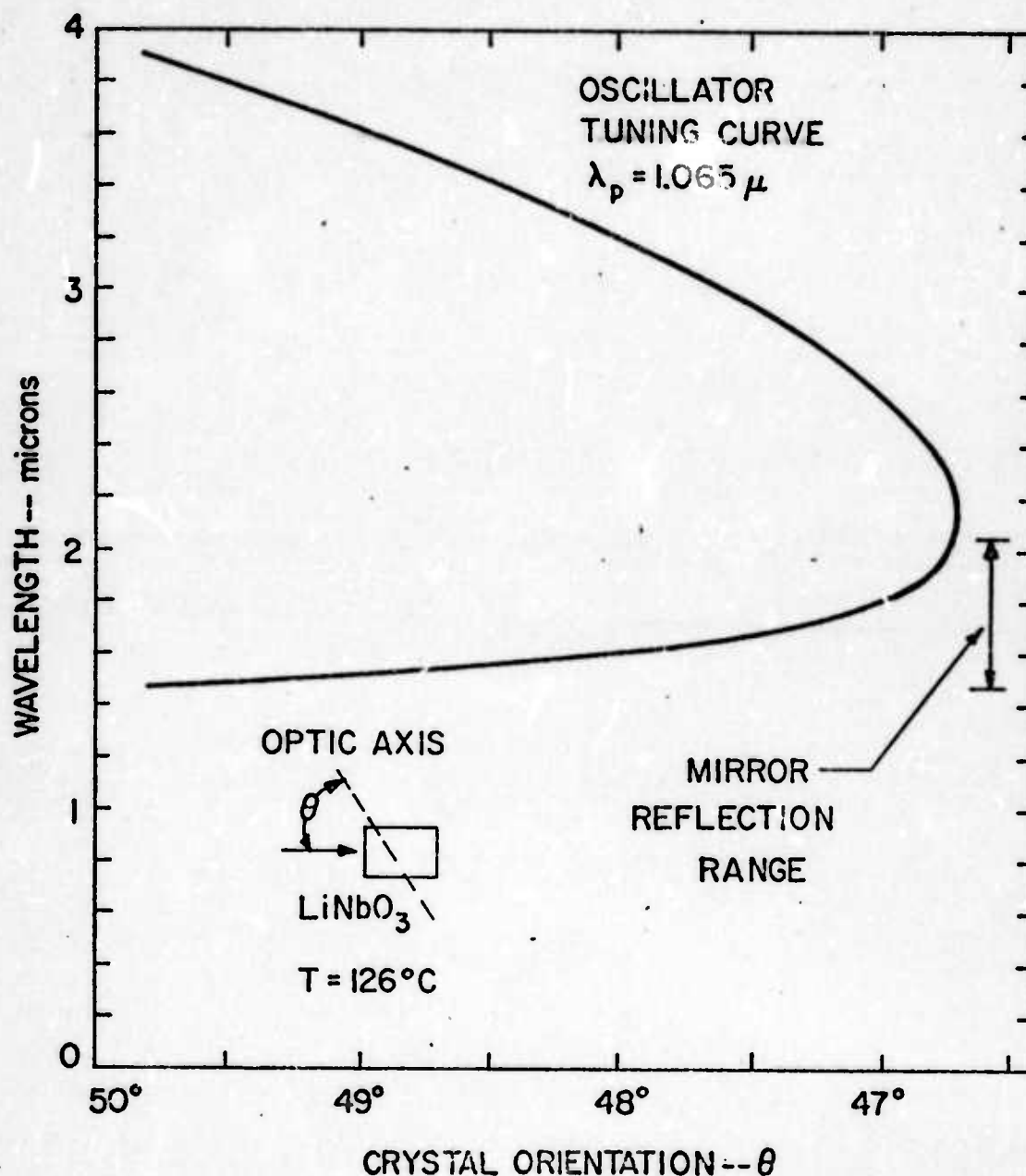


FIG. 3--Tuning curve for the LiNbO<sub>3</sub> parametric oscillator vs. crystal angle. The mirror reflectance range is indicated.

The gain of a parametric amplifier is given by<sup>2</sup>

$$G = \Gamma^2 l^2 = \left( \frac{2\omega_0^2 d^2}{\pi n_0^2 n_3 \epsilon_0 c^3} \right) P_{30} l k_0 (1 - \delta^2)^2 \bar{h}(B, \xi) \quad (1)$$

In the plane wave limit with  $B = 0$

$$\bar{h}(0, \xi) \rightarrow \xi = l/b \quad (2)$$

so that

$$\begin{aligned} G = \Gamma^2 l^2 &= \left( \frac{\omega_0^2 d^2}{n_0^2 n_3 \epsilon_0 c^3} \right) P_{30} \frac{2l}{\pi} k_0 (1 - \delta^2)^2 \frac{l}{b} \\ &= \frac{K P_{30} l^2 (1 - \delta^2)^2}{(\pi w_0^2/2)} = \frac{K P_{30} l^2 (1 - \delta^2)^2}{A} \end{aligned} \quad (3)$$

since

$$\frac{b}{k_0} = w_0^2 \quad (4)$$

and for Gaussian beams

$$A = \frac{\pi w_0^2}{2} \quad (5)$$

For double refraction limited focusing

$$\bar{h}(B, \xi) \approx \frac{\bar{h}_{\text{mm}}(0)}{1 + l/l_{\text{eff}}} \approx l_{\text{eff}}/l \quad (6)$$

In this case the gain as a function of power is independent of crystal length. However, the gain does improve with  $l^2$  as a function of intensity since

$$\frac{\pi w_0^2}{2} = \frac{\pi}{16} \rho^2 l^2 \quad (7)$$

is the useful maximum focal area. The effective interaction length is

$$l_{\text{eff}} = \frac{\lambda_0}{2n_0 \rho^2} \bar{h}_{\text{mm}}(0) \approx \frac{\lambda_0}{2n_0 \rho^2} \quad (8)$$

When the focal area determined by the crystal damage intensity equals that given by walk-off considerations, the use of  $90^\circ$  phasematched crystals is no longer required to maximize gain. Figure 4 shows the damage limited focal area. Also plotted are the  $90^\circ$  phasematched areas for a 5 cm crystal and the areas for  $45^\circ$  phasematched crystals of various lengths.

For areas greater than the walk-off area at a given crystal length, the plane wave gain formula applies. Thus for a 2 cm crystal, 1 mJ of energy is required at  $1 \text{ J/cm}^2$  damage limit to reach the plane wave gain.

In this limit of loose focusing

$$\bar{h}(B, \xi) = \frac{l/b}{1 + l/l_{\text{eff}}} \approx l/b \quad (9)$$

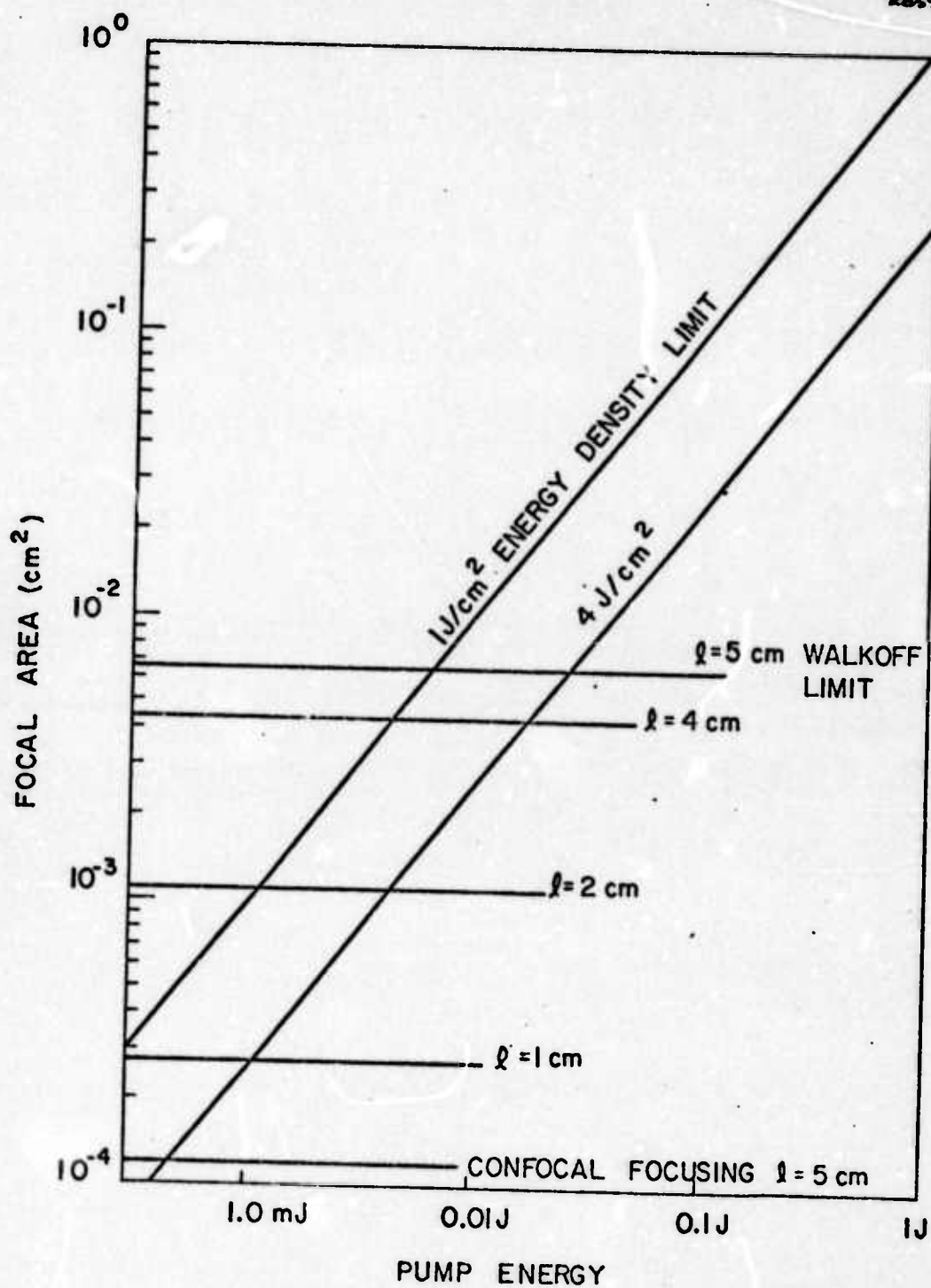


FIG. 4--Damage limited focal areas vs. input pump energy for  $\text{LiNbO}_3$ . The plane wave gain approximation applies for input energies greater than 8 mJ at  $l = 5$  cm.



so that the gain reduces to

$$G = \frac{K P_{30} l^2 (1 - \delta^2)^2}{(\pi \omega_0^2 / 2)} \quad (10)$$

for both  $90^\circ$  and off-angle phasematched crystals. For example, for 5 cm long crystals the gain is maximum at 0.1 mJ for  $1 \text{ J/cm}^2$  damage threshold at  $90^\circ$  phasematching. For  $45^\circ$  phasematching, the gain is maximum for energies greater than 8 mJ. At this energy, the gain for off-angle phasematching equals that of  $90^\circ$  phasematching for the limiting input intensity and there is no requirement for the use of  $90^\circ$  crystals.

The calculated gain for the parametric oscillator is  $\Gamma^2 l^2 = 0.32$  at  $1 \text{ MW/cm}^2$  for a 5 cm crystal. At the  $80 \text{ MW/cm}^2$  burn-density limit, the parametric oscillator gain at degeneracy is

$\Gamma^2 l^2 = 1.0$	$l = 1 \text{ cm}$
$= 4.0$	$= 2 \text{ cm}$
$= 9.0$	$= 3 \text{ cm}$
$= 16.0$	$= 4 \text{ cm}$
$= 25.0$	$= 5 \text{ cm}$

For efficient operation, gains greater than 4 are adequate. Presently available  $\text{LiNbO}_3$  y-axis boules allow crystal lengths up to 5.0 cm. For longer crystals, special boules can be grown either along the y-axis or in the  $(01\bar{4})$  direction. We have recently evaluated a  $(01\bar{4})$  grown boule

and have shown that quality crystals up to 5 cm in length are available at  $49^\circ$  phasematching angle.

The important conclusion reached here for the first time, is that parametric oscillator operation at  $45^\circ$  phasematching has the same gain characteristic as  $90^\circ$  phasematched operation for pump energies greater than 10 mJ. The electro-optic Q-switched Nd:YAG laser source meets this requirement even without the following amplifier. The amplifier does provide a significant increase in output energy that may improve the usefulness of this source for certain experiments. It is, however, not required for the successful operation of the widely tunable device.

Rise time considerations due to the short pump pulse length dictate a short oscillator cavity. However, since the equivalent loss due to rise time varies as cavity length, and the gain varies as  $I^2$ , it is advantageous to use the longest available crystal lengths.<sup>2</sup>

The output of the parametric oscillator tunes between  $1.5\mu$  and  $3.7\mu$  using a single set of reflecting optics. This basic frequency range can be extended to cover the  $3\mu$  to  $18\mu$  region in  $\text{AgGaSe}_2$  and the  $10\mu$  to  $27\mu$  region in  $\text{CdSe}$ . Various sum generation processes also are possible in  $\text{LiNbO}_3$  and  $\text{LiIO}_3$ . For example, the SHG of the idler in  $\text{LiNbO}_3$  covers the  $1.06\mu \rightarrow 1.6\mu$  region, and the SHG of the signal in  $\text{LiNbO}_3$  covers the  $0.75\mu \rightarrow 1.06\mu$  region. These processes angle phasematch and should be  $\sim 30\%$  efficient. In addition,  $1.06 + \text{idler}$  in  $\text{LiNbO}_3$  and  $1.06 + \text{signal}$  in  $\text{LiNbO}_3$  cover the  $0.7\mu \rightarrow 0.8\mu$  and  $0.6\mu \rightarrow 0.7\mu$  spectral range. Due to the high  $1.06\mu$  power available these steps are also efficient. The above steps all involve a single angle phasematched  $\text{LiNbO}_3$  crystal. There may not be any

requirement to generate wavelengths shorter than  $6000 \text{ \AA}$  ; however, by use of a second crystal to sum the oscillator and its second harmonic in  $\text{LiIO}_3$ , the spectral range from  $3300 \text{ \AA}$  to  $7000 \text{ \AA}$  can also be covered. Figure 5 illustrates the spectral range versus phasematching angle reached by the  $\text{LiNbO}_3$  parametric oscillator and the following mixers and sum generators.

For infrared generation by mixing we consider the  $\text{LiNbO}_3$  parametric oscillator as a source of radiation at the signal and idler frequencies. The output energy of the oscillator at degeneracy is assumed to be 30% the input pump energy. Two output energy ranges are possible, 3 mJ per pulse without the Nd:YAG amplifier, and 100 mJ per pulse with the Nd:YAG amplifier. Table I shows the estimated output power versus parametric oscillator frequency at the signal and idler waves.

The conversion efficiency for parametric mixing is given by

$$\left( \frac{\omega_1}{\omega_2} \right) \Gamma^2 I^2 = \frac{P_1}{P_2} \left( \frac{\omega_{1R}}{\omega_p} \right) = \left( \frac{\omega_1}{\omega_2} \right) \frac{2\omega_1\omega_2 |d|^2 I_3^2}{n_1 n_2 n_3 \epsilon_0 c^3} \quad (11)$$

where  $\omega_1$  = infrared output,  $\omega_2$  = idler frequency, and  $\omega_3$  = signal frequency.

For CdSe and  $\text{AgGaSe}_2$ , the conversion efficiency for a pump wavelength at  $1.833\mu$  is given by

$$\Gamma^2 I^2 \left( \frac{1\text{MW}}{\text{cm}^2} \right) \text{ CdSe} = 0.006 \quad l = 1 \text{ cm}$$

$$\Gamma^2 I^2 \left( \frac{1\text{MW}}{\text{cm}^2} \right) \text{ AgGaSe}_2 = 0.020 \quad l = 1 \text{ cm}$$

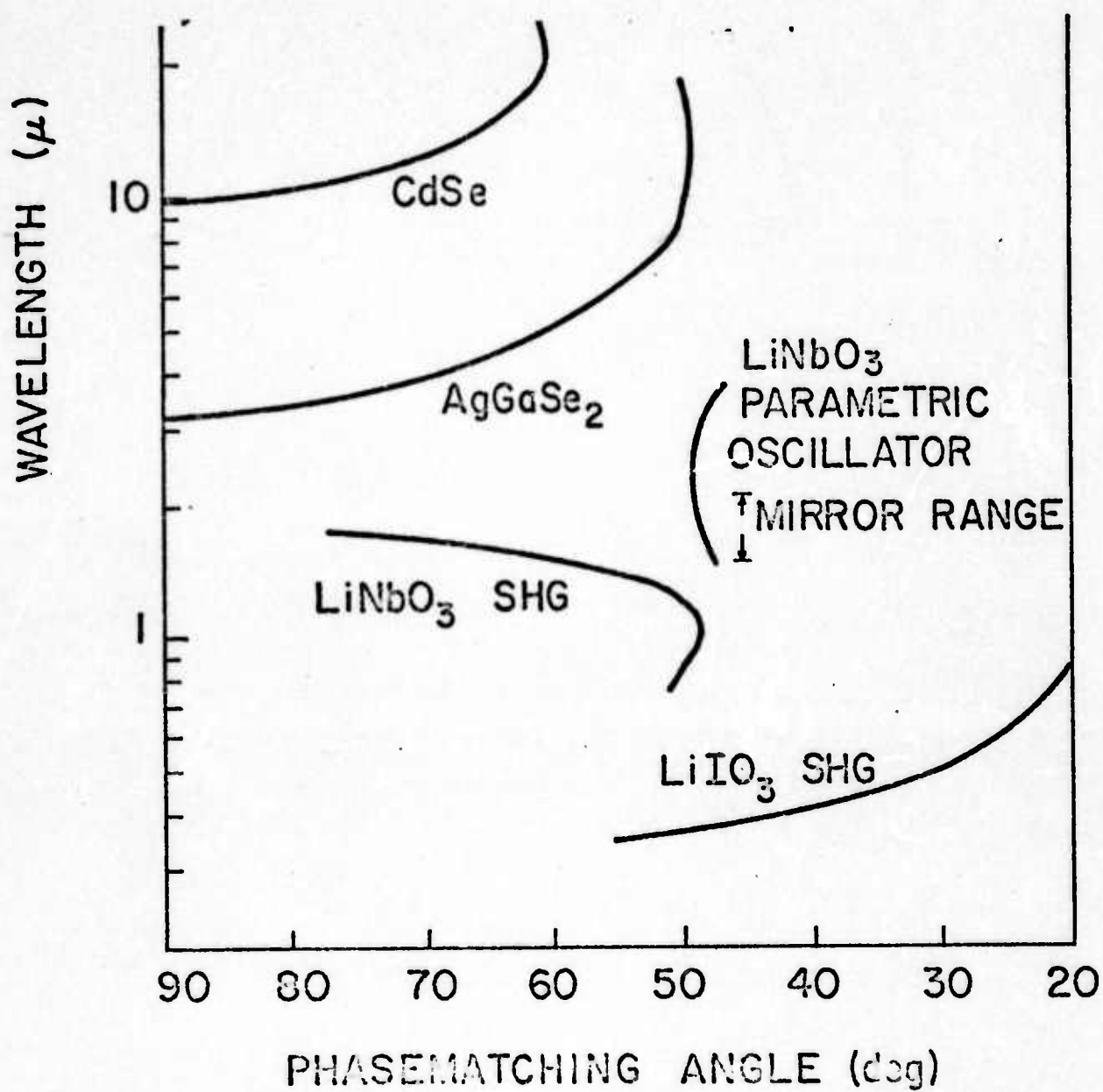


FIG. 5--Spectral range vs. crystal angle for the LiNbO<sub>3</sub> oscillator and following nonlinear crystal harmonic, sum, and mixer generators.

TABLE I  
Estimated Output Energy of the  $\text{LiNbO}_3$  Parametric Oscillator Source

WAVELENGTH	10 mJ PUMP	300 mJ PUMP.
1.5 $\mu$	2.12 mJ	70.5 mJ
1.6 $\mu$	2.00	66.5
1.8 $\mu$	1.75	58.2
2.1 $\mu$ (deg)	3.00 mJ (s + i)	100.0 mJ (s + i)
2.5 $\mu$	1.27	42.0
3.0 $\mu$	1.06	35.0
3.5 $\mu$	0.91	30.0



for phasematching near the  $60^\circ$  direction. In either crystal walk-off is not a problem so that  $I_3$  is limited by the crystal burn density. For CdSe  $I_3 \lesssim 50 \text{ MW/cm}^2$  and for AgGaSe<sub>2</sub>  $I_3 \lesssim 10 \text{ MW/cm}^2$ . The maximum conversion efficiencies are therefore

$$\Gamma^2 I_{\text{MAX}}^2 (\text{CdSe}) = 30\% \quad l = 1 \text{ cm}$$

$$\Gamma^2 I_{\text{MAX}}^2 (\text{AgGaSe}_2) = 20\% \quad l = 1 \text{ cm}$$

This improves as  $l^2$  in the present focusing limit. The actual output energy per pulse versus wavelength is shown in Table II.


Mixing in AgGaSe<sub>2</sub> and CdSe is straightforward.<sup>3,4</sup> The only requirement is for proper crystal phasematching by angular rotation. Figure 6 shows the phasematching peak obtained by mixing  $1.318\mu$  and a  $0.659\mu$  pumped LiNbO<sub>3</sub> parametric oscillator in AgGaSe<sub>2</sub>. The width of the peak is  $24 \text{ cm}^{-1}$  at  $1000 \text{ cm}^{-1}$ . Figure 7 shows the measured mixed output wavelengths of this device when the parametric oscillator is tuned. In the present mixer, a single crystal cut at  $62^\circ$  phasematches over the  $3.5\mu$  to  $18\mu$  spectral range, as illustrated in Fig. 5.

CdSe also phasematches over its entire useful range with the use of a single crystal cut at  $70^\circ$ . Due to lack of transparency and birefringence,  $27\mu$  is the longest phasematched wavelength generated in the mid-infrared.

The angular tolerance for phasematching is large enough that mechanical or simple electrical tracking is possible without active feedback

TABLE II

Expected Output Energies for Mixing in CdSe and AgGaSe<sub>2</sub>

INPUT WAVELENGTHS		OUTPUT WAVELENGTHS		OUTPUT ENERGY (10 mJ)	OUTPUT ENERGY (300 mJ)
AgGaSe <sub>2</sub> $l = 1 \text{ cm}$ $\Gamma^2 l^2 = 20\%$					
1.65 $\mu$	3.05 $\mu$	3.5 $\mu$	$\theta = 75^\circ$	0.18 mJ	6.0 mJ
1.70	2.90	4.0	$\theta = 68^\circ$	0.15	5.0
1.75	2.70	5.0	$\theta = 62^\circ$	0.12	4.0
1.85	2.50	7.0	$\theta = 52^\circ$	0.09	3.0
1.95	2.35	10.0	$\theta = 49^\circ$	0.07	2.1
CdSe $l = 1 \text{ cm}$ $\Gamma^2 l^2 = 30\%$					
1.95 $\mu$	2.35 $\mu$	10.0 $\mu$		0.10	3.5
	degenerate	15.0		0.063	2.1
		20.0		0.044	1.5
		25.0		0.04	1.2

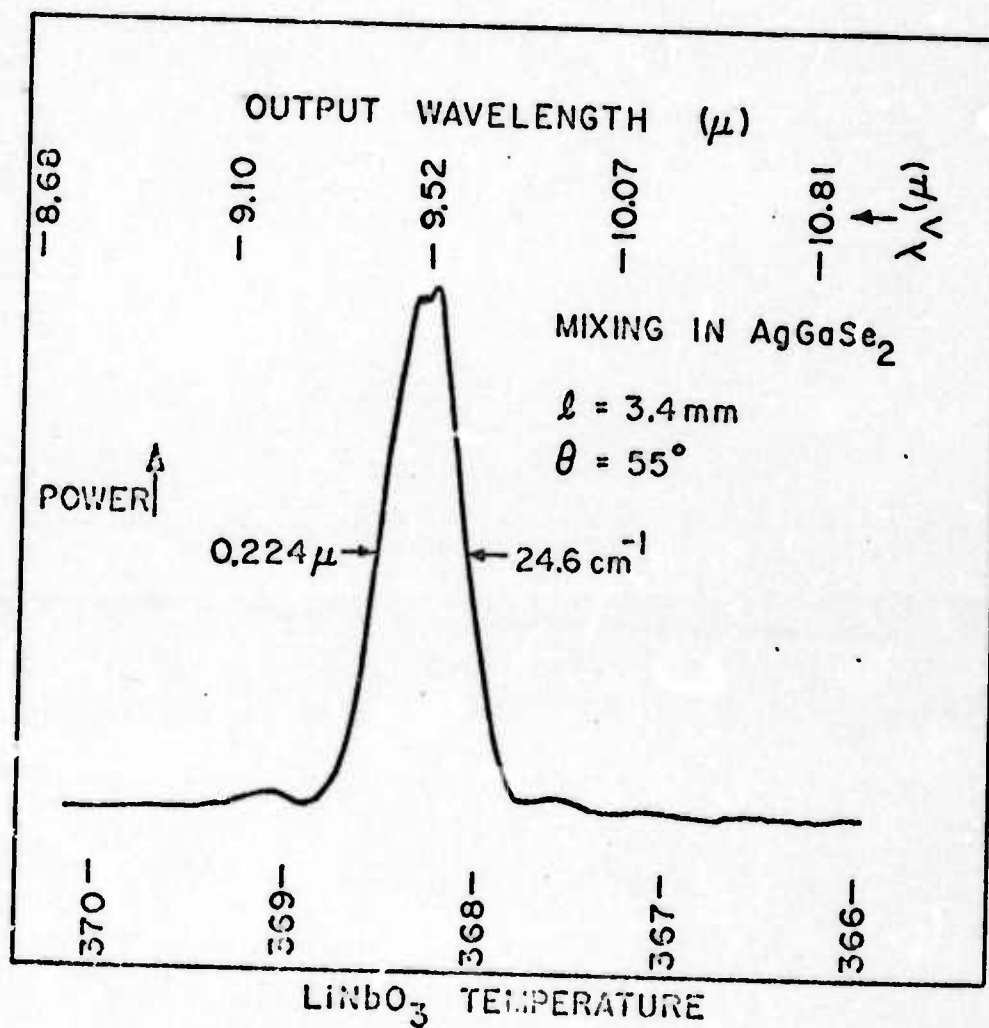


FIG. 6--Phasematching peak for mixing in  $\text{AgGaSe}_2$ .

2808-3

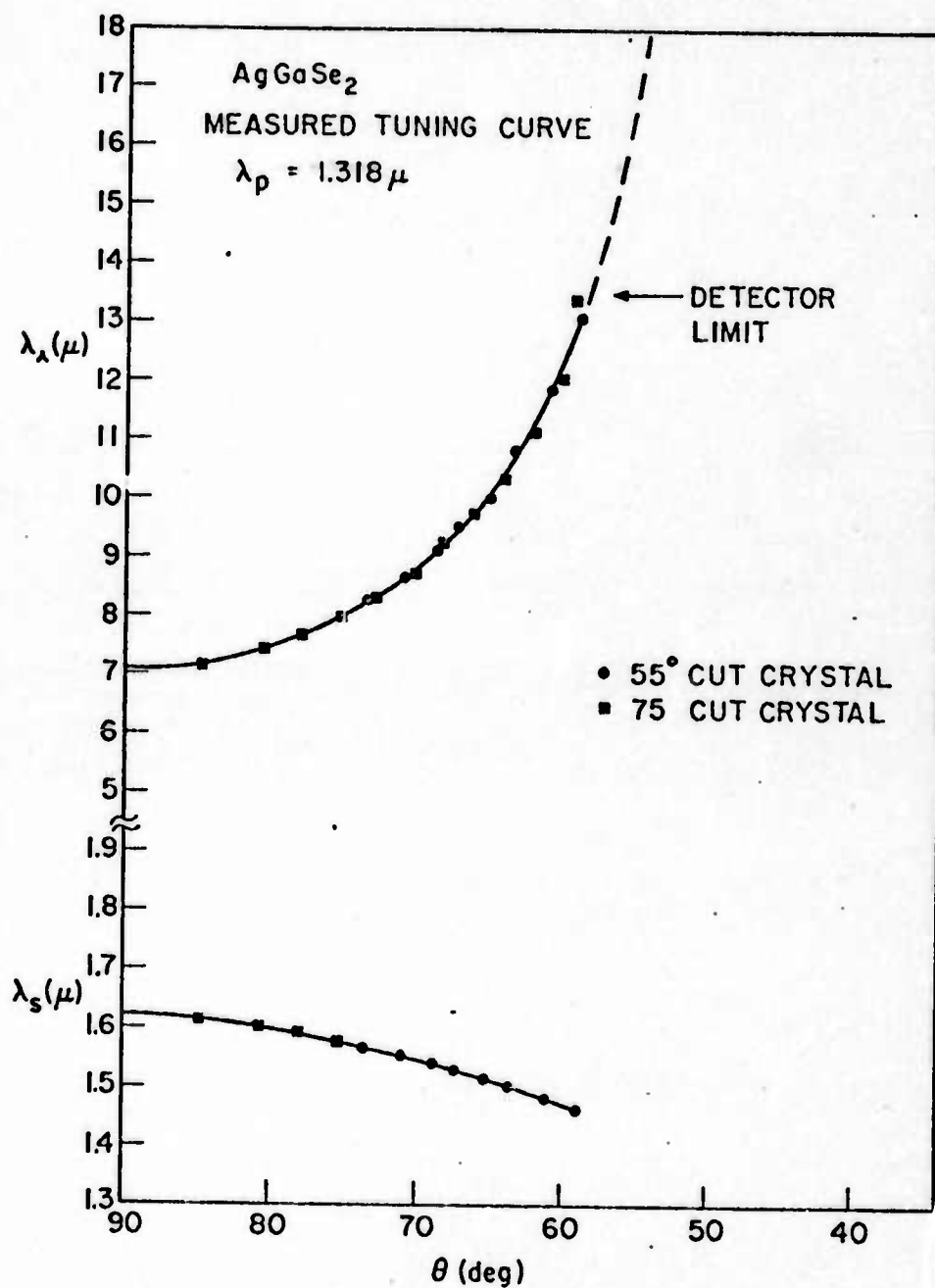


FIG. 7--Measured output wavelength for mixing 1.32 $\mu$  and a LiNbO<sub>3</sub> parametric oscillator in AgGaSe<sub>2</sub>.

stabilization. To minimize optical components, the mixing crystals are rotated about an axis  $45^\circ$  to the vertical. In this way half of the oscillator output is properly polarized for mixing. The mixed output can be selected with an InAs filter for both  $\text{AgGaSe}_2$  and  $\text{CdSe}$ .

The possible methods of extending the parametric oscillator wavelength into the visible are discussed next. The conversion efficiencies are calculated for second harmonic generation in  $\text{LiNbO}_3$ ,  $\text{LiIO}_3$ , and KDP. Since the oscillator covers a tuning range greater than two to one, there are no gaps in the generated sum and harmonic spectrum.

Second harmonic generation in  $\text{LiNbO}_3$  phasematches for fundamental wavelengths between  $1.2\mu$  and  $3.6\mu$ . The angle tuning curve for SHG of the parametric oscillator signal and idler is shown in Fig. 5. For SHG the input polarization is ordinary and the output is extraordinary. A polarizer and filter can be used to filter the fundamental from the generated harmonic. The conversion efficiency to the harmonic equals the gain of the oscillator or

$$\Gamma^2 l^2 = \frac{P_{\text{SH}}}{P_{\text{F}}} = 1 \quad \begin{array}{l} l = 1 \text{ cm} \\ \lambda = 2.1\mu \\ I = 80 \text{ MW/cm}^2 \end{array}$$

Thus for a crystal 2 cm in length, the second harmonic conversion is well into the nonlinear conversion limit given by  $\tanh^2(\Gamma l)$ . In practice, external SHG of a plane wave source results in a conversion efficiency of



between 30% - 50%. Assuming a 40% conversion efficiency, the generated SH energies are listed in Table III.

According to Fig. 4, the plane wave focusing limit applies for input energies  $> 1$  mJ for 2 cm crystals, and  $> 8$  mJ for 5 cm crystals. Therefore, the 10 mJ Nd:YAG pump source provides adequate parametric oscillator energy for efficient second harmonic generation.

Sum generation in  $\text{LiNbO}_3$  against the  $1.06\mu$  pump also phasematches. In this case good efficiency is possible due to the 7 mJ and 200 mJ of  $1.06\mu$  energy available. For sum generation the conversion efficiency in the low gain limit is again  $\Gamma^2 l^2$ . For high conversion efficiencies

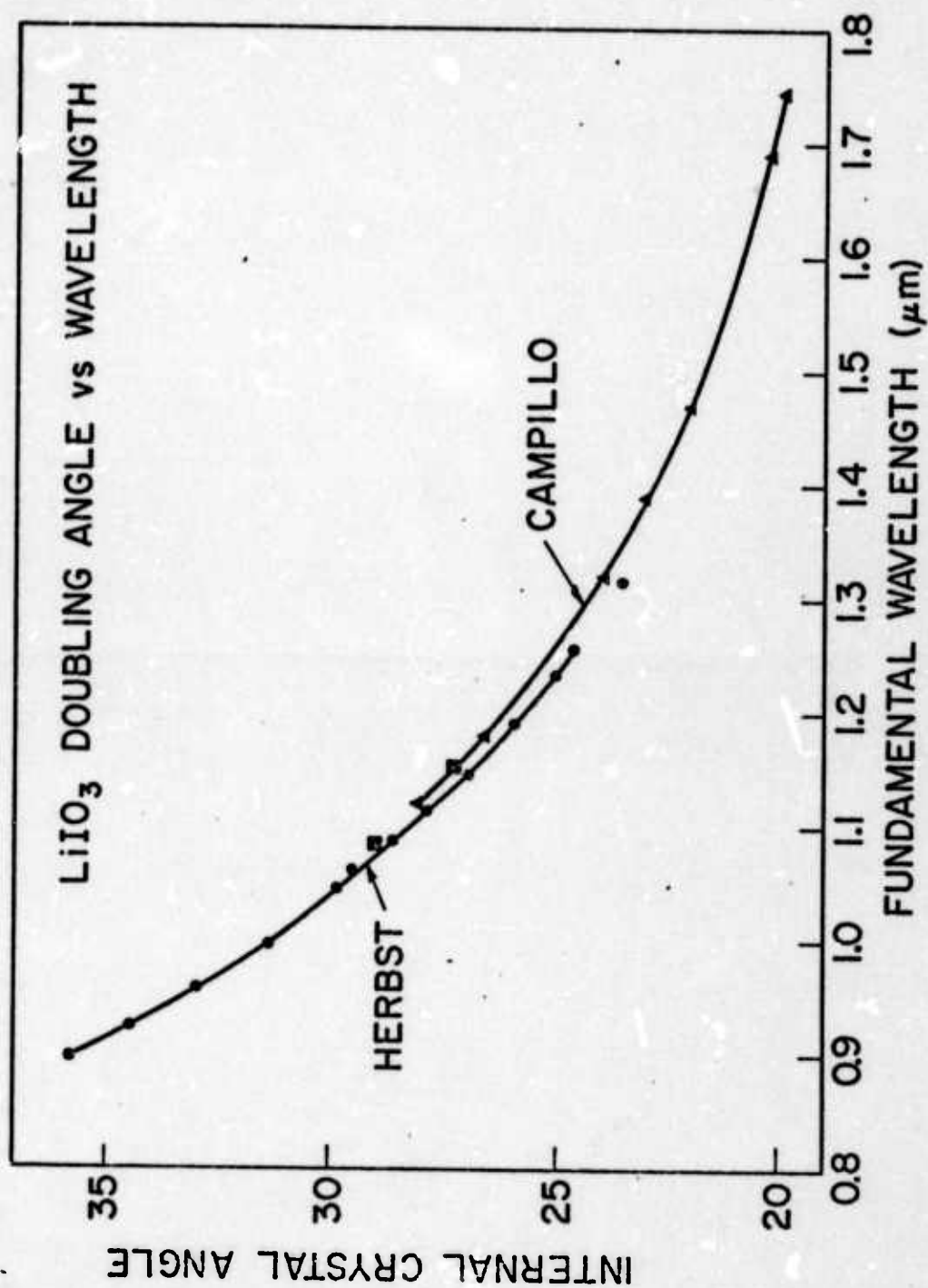
$$\frac{P_{\text{SUM}}}{P_{\text{IN}}} = \left( \frac{\omega_{\text{SUM}}}{\omega_{\text{IN}}} \right) \sin^2 \Gamma l$$

Since  $\Gamma l \gtrsim 1$  it is expected that all of the oscillator energy can be up-converted to the  $0.618 \rightarrow 0.82\mu$  spectral region. In summary, the oscillator can be up-converted to a wavelength region between  $0.62\mu$  and  $1.5\mu$  with a single angle phasematched crystal of  $\text{LiNbO}_3$ . This spectral range is important since it cannot be directly reached by other tunable sources such as diode lasers or dye lasers.

For generation of shorter visible and ultraviolet wavelengths down to  $3500 \text{ \AA}$ ,  $\text{LiIO}_3$  can be used as a nonlinear crystal. Figure 8 shows the phasematching angles for SHG in  $\text{LiIO}_3$ . Figure 5 shows the phasematching angles for SHG of the doubled parametric oscillator. It is informative to determine the required pump energy for high conversion efficiency in  $\text{LiIO}_3$ .

TABLE III  
Generated Second Harmonic Energies

S.H. WAVELENGTH	10 mJ PUMP	300 mJ PUMP
0.75 $\mu$	0.85	28.0
0.80 $\mu$	0.80	26.0
0.90 $\mu$	0.70	23.0
1.0 $\mu$	0.60	20.0
1.2 $\mu$	0.51	16.8
1.5 $\mu$	0.42	14.0
1.7 $\mu$	0.35	12.0

FIG. 8--Measured SHG phasematching angles for LiIO<sub>3</sub>.

The conversion efficiency in  $\text{LiIO}_3$  is

$$\begin{aligned}\Gamma^2 l^2 &= 0.0055 \left( \frac{1 \text{ MW}}{\text{cm}^2} \right) & l &= 1 \text{ cm} \\ & & \lambda_f &= 1.4 \mu \\ &= 0.022 \left( \frac{\text{MW}}{\text{cm}^2} \right) & l &= 1 \text{ cm} \\ & & \lambda_f &= 0.69 \mu\end{aligned}$$

For a 1 cm crystal, the walk-off limited focal area is

$$\begin{aligned}\frac{\pi \omega_0^2}{2} &= \frac{\pi}{16} \rho^2 l^2 & \rho &= 0.07 \\ &= 10^{-3} \text{ cm}^2 & l &= 1 \text{ cm}\end{aligned}$$

The burn density of  $\text{LiIO}_3$  is  $100 \text{ MW/cm}^2$ . Therefore, the conversion efficiency is

$$\Gamma^2 l^2 \left( \frac{100 \text{ MW}}{\text{cm}^2} \right) = 0.55 \quad \lambda_f = 1.4 \mu$$

and

$$\Gamma^2 l^2 \left( \frac{100 \text{ MW}}{\text{cm}^2} \right) = 2.2 \quad \lambda_f = 0.69 \mu$$

at an input power greater than 0.1 MW or an input energy greater than 2 mJ per pulse. Table III shows that the 10 mJ Nd:YAG source results in output energies near 0.8 J at the SH of the oscillator. Thus SHG

in 1 cm of  $\text{LiIO}_3$  will be limited to near 20% efficiency. For the 300 mJ pump source, adequate energy is available for efficient ( $\sim 30\%$ ) SHG of the doubled parametric oscillator. The wavelength range is therefore extended to  $3300 \text{ \AA}$  by two crystals of  $\text{LiIO}_3$  cut for proper angular phasematching.

Second harmonic generation in angle phasematched KDP has been considered in detail in a short unpublished note.<sup>4</sup> The important parameters are summarized here for completeness. Figure 9 shows the phasematching angles for KDP and ADP. Wavelengths down to  $2600 \text{ \AA}$  are phasematched by SHG and down to  $2200 \text{ \AA}$  by sum generation of the fourth harmonic of  $1.06\mu$  and tunable radiation near  $1\mu$ .<sup>5</sup>

Figure 10 shows the calculated SHG efficiency in KDP for a 1 cm length crystal versus input intensity. For harmonic generation between  $5200 \text{ \AA}$  and  $6000 \text{ \AA}$

$$\frac{P_{\text{SH}}}{P_{\text{F}}} = 8 \times 10^{-4} \rightarrow 4 \times 10^{-3} \left( \frac{1\text{MW}}{\text{cm}^2} \right) \quad l = 1 \text{ cm}$$

The burn density of KDP is greater than  $500 \text{ MW/cm}^2$  so that for optimum off-angle focusing given by

$$\begin{aligned} \frac{\pi \omega_0^2}{2} &= \frac{\pi}{16} \rho^2 l^2 & \rho &= 0.03 \\ &= 1.64 \times 10^{-4} \text{ cm}^2 & l &= 1 \text{ cm} \end{aligned}$$



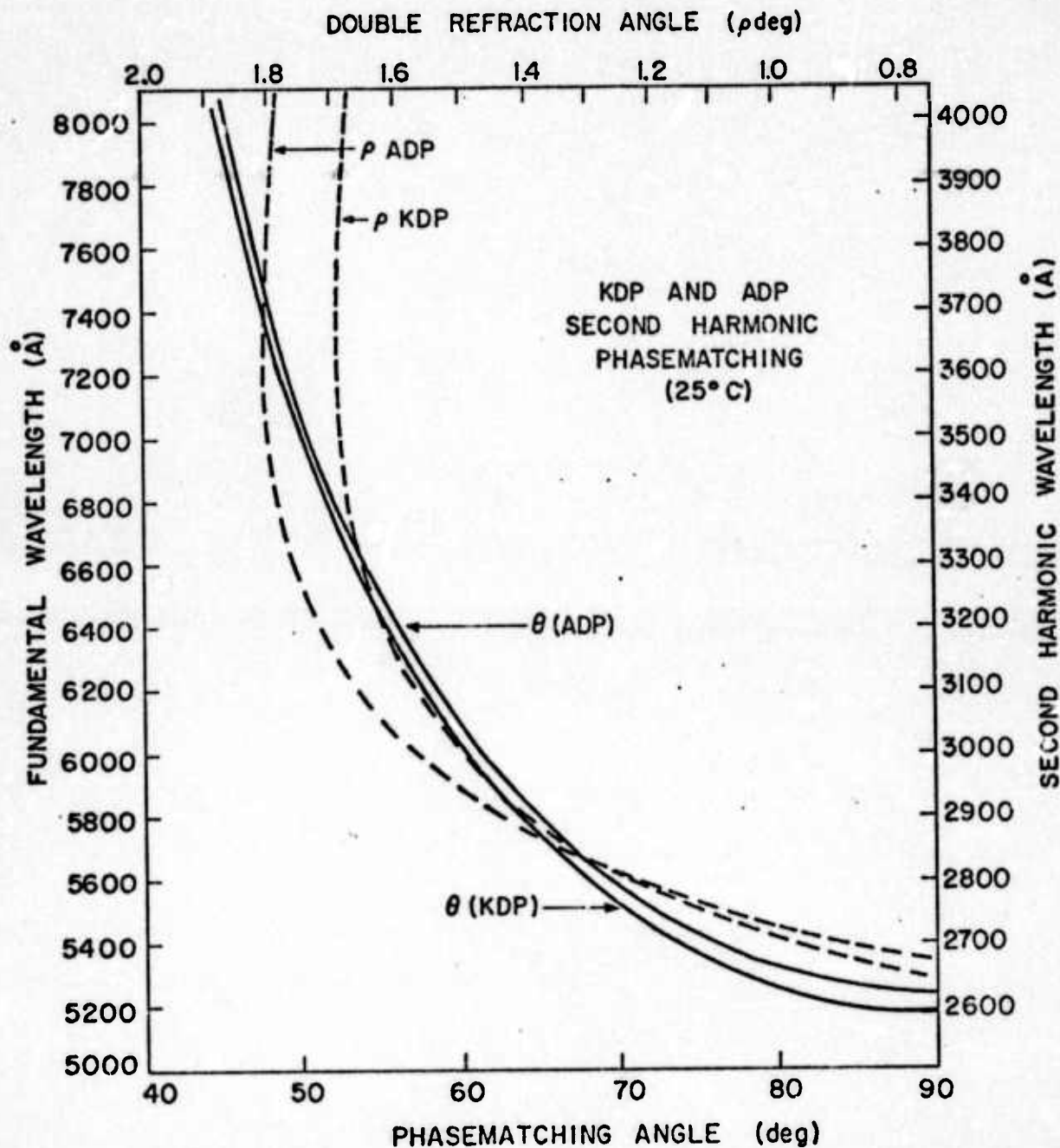


FIG. 9--Phase-matching angles for KDP and ADP.

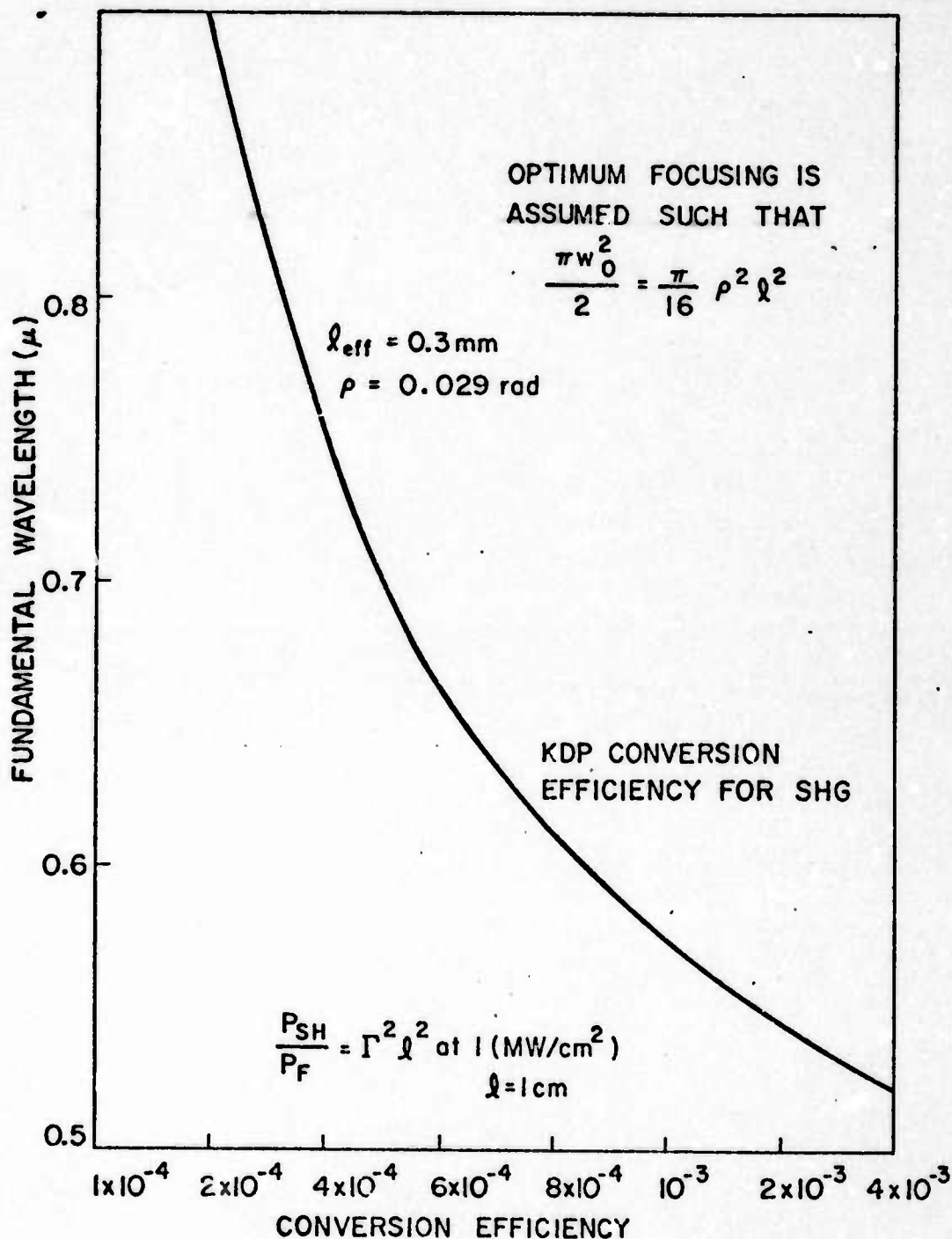


FIG. 10--Calculated SHG efficiency in KDP vs. pump wavelength.

the required peak power to achieve the burn density limit is

$$P_{\text{pump}} = 80 \text{ kW}$$

The conversion constant is thus

$$\Gamma^2 l^2 = 0.40 \rightarrow 2.0 \quad l = 1 \text{ cm}$$

At 80 kW and 15 nsec the required pump energy is 1.2 mJ . Again, efficient conversion to the ultraviolet is possible with the 300 mJ Nd:YAG pump source. With the 10 mJ pump source sum generation against the second harmonic of the pump must be used to achieve efficient conversion.

In summary, the generation of visible and near ultraviolet is a useful extension of the efficient widely tunable infrared parametric oscillator source. The  $\text{LiNbO}_3$  SHG step is expected to be near 30% efficiency for wavelengths in the  $6100 \text{ \AA}$  to  $1.5\mu$  region.  $\text{LiIO}_3$  can be used to extend the generated wavelengths to  $3300 \text{ \AA}$  . Beyond the near ultraviolet either KDP or ADP can be used. The conversion efficiency can be increased by using sum and mixing against the harmonics of  $1.06\mu$  . The shortest wavelength that phasematches is  $2200 \text{ \AA}$  in ADP reached by sum generation of the fourth harmonic of  $1.06\mu$  at  $2660 \text{ \AA}$  and a tunable source near  $1\mu$  .

The  $1.06\mu$  Nd:YAG laser pumped  $\text{LiNbO}_3$  parametric oscillator forms a nearly ideal primary source for widely tunable  $2200 \text{ \AA}$  to  $1.5\mu$  radiation by second harmonic and sum generation,  $1.5\mu$  to  $3.7\mu$  by parametric oscillation, and  $3.0\mu$  to  $27\mu$  by phasematched mixing.

In this section we have described a unique widely tunable, high energy, pulsed, tunable coherent source. The device is based on an angle tuned  $1.06\mu$  pumped  $\text{LiNbO}_3$  parametric oscillator whose features are described for the first time. The oscillator's basic  $1.5\mu$  to  $3.7\mu$  frequency range is extended toward the infrared by mixing in  $\text{AgGaSe}_2$ ,  $\text{CdSe}$ , and  $\text{LiNbO}_3$ . It is extended to the visible and ultraviolet by second harmonic and sum frequency generation in  $\text{LiNbO}_3$ ,  $\text{LiIO}_3$ , and KDP. The parametric oscillator source is conservatively estimated to be 30% efficient when pumped with a 10 mJ per pulse or 300 mJ per pulse Nd:YAG laser. Similarly, the following mixing and sum generation steps are also shown to be near 30% efficient. The parametric oscillator followed by a crystal of  $\text{AgGaSe}_2$ ,  $\text{CdSe}$ , and  $\text{LiNbO}_3$  thus efficiently tunes over a spectral range between  $0.62\mu$  and  $27\mu$ . Since all processes are angle phase-matched, the tuning rate can be rapid.

The gain bandwidth of the oscillator is near  $10\text{ cm}^{-1}$ . The oscillator can be frequency narrowed by use of two internal etalons or a birefringent crystal plus etalon. It is expected that continuous scanning with  $1\text{ cm}^{-1}$  resolution is possible. For higher resolution, the tuning range is approximately  $1\text{ cm}^{-1}$ , and for single mode operation near  $0.1\text{ cm}^{-1}$ , the oscillator cavity free spectral range. The use of continuous helium-neon lasers for frequency stabilization is described, as are possible methods of convenient frequency measurement.

The combination of wide tuning range at high pulse energies is a unique feature of the tunable coherent source described in this paper. At this time, no other single device approaches these features. In

addition, the Nd:YAG pump laser and all optical and nonlinear optical elements operate at or slightly above room temperature and have no inherent properties that limit the useful operating life with the exception of the flashlamps used to pump the Nd:YAG laser and amplifier. Based on present lifetime data, the flashlamps last to  $10^7$  pulses or over 100 days of continuous operation at 10 pps. Thus in addition to its unique spectral properties, the system described here has inherently long operational life with minimum required maintenance.



## REFERENCES

1. M. Yarborough, private communication.
2. R. L. Byer, "Optical Parametric Oscillators," Treatise in Quantum Electronics (H. Rabin and C. L. Tang, eds.), Academic Press, New York (to be published).
3. R. L. Herbst and R. L. Byer, "Efficient Parametric Mixing in CdSe," Appl. Phys. Letters 19, 527 (December 1971).
4. R. L. Byer, M. Choy, R. L. Herbst, D. S. Chemba, and R. S. Feigelson, "Second Harmonic Generation and Infrared Mixing in  $\text{AgGaSe}_2$ ," IEEE J. Quant. Elect. (to be published).
5. R. L. Byer, "SHG in KDP and ADP".
6. R. L. Herbst, "Sum Generation in ADP".

### III. GENERATION OF VACUUM ULTRAVIOLET AND SOFT X-RAY RADIATION

During the past report period the following work has been achieved on this project: (a) we have successfully generated the shortest coherent radiation to date at  $887 \text{ \AA}$  via third harmonic generation of  $2660 \text{ \AA}$  radiation in argon; (b) we have developed a theory on higher-order polarizabilities; and (c) we have proposed an experiment for the generation of radiation below  $300 \text{ \AA}$ .

A schematic of the experimental set-up for generating  $887 \text{ \AA}$  radiation is shown in Fig. 1. A single 30 psec wide pulse is switched out of a train of mode-locked Nd:YAG laser pulses and is frequency doubled twice in successive KDP crystals to  $2660 \text{ \AA}$ . The available power at  $2660 \text{ \AA}$  is  $\sim 5 \times 10^7$  watts peak. This radiation is focused to a spot size of  $35 \text{ }\mu\text{m}$  in diameter at the output end of the gas cell. The nonlinear media was Ar at a pressure of 20 Torr. Since no window material is transparent at this wavelength, differential pumping was used between the cell exit and the entrance to the VUV spectrometer. Detection was done with a Xe ionization chamber. At an incident power density of  $10^{13} \text{ W/cm}^2$ , the observed conversion efficiency was only  $10^{-7}$  and the signal was too low to allow a determination of whether Ar is positively or negatively dispersive for this process.

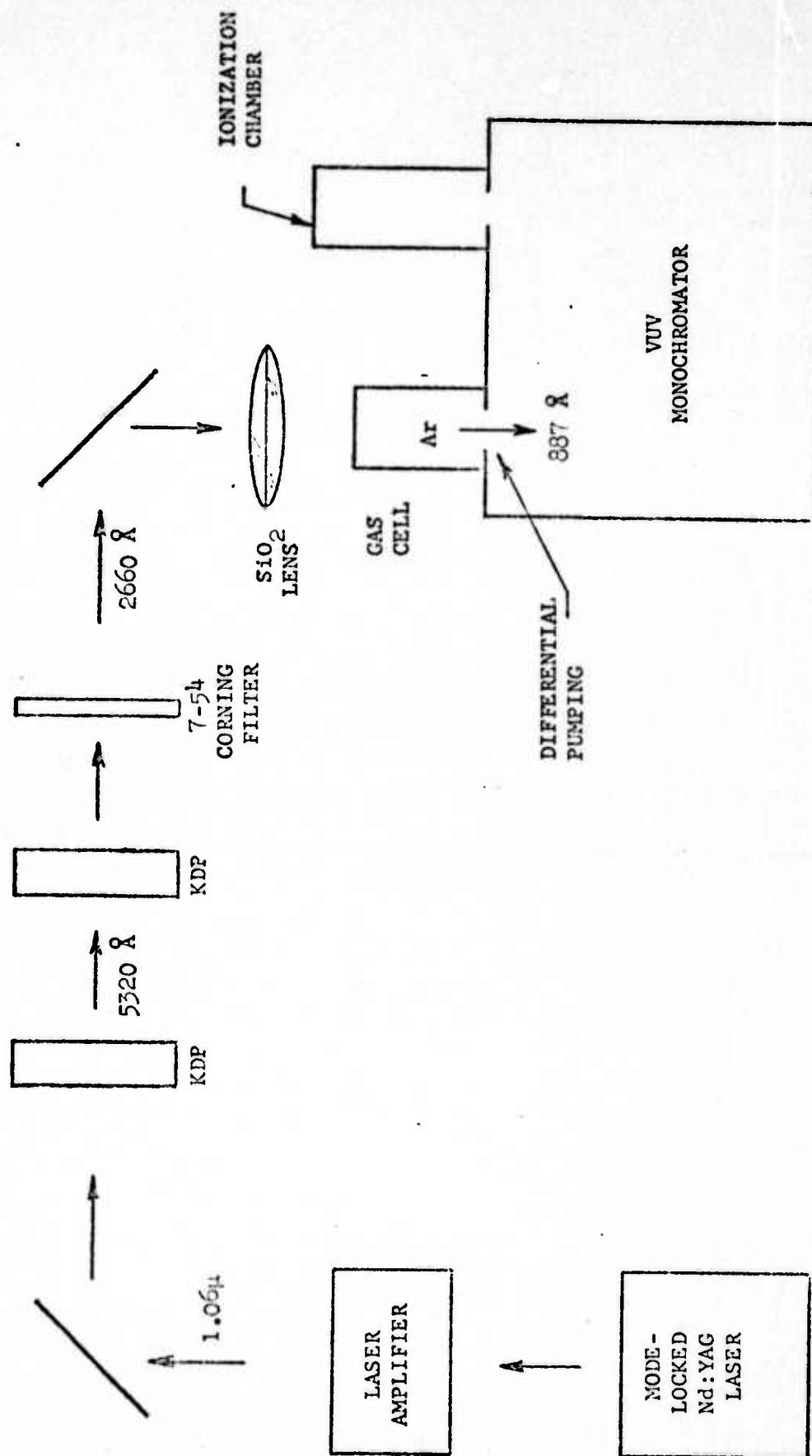


FIG. 1--Experimental set-up for generation of 887 Å radiation.

To extend nonlinear optical techniques into the soft x-ray region, we considered the use of higher-order nonlinear optical polarization which might allow fifth, seventh, or higher order harmonic generation. We used the density matrix approach to examine the relative magnitude of higher-order polarizations subject to the condition that the applied electric field strength does not exceed the multi-photon absorption or ionization limit. Analysis shows that if the generated frequency is sufficiently close to an upper level of the atom that this level determines both the coherence length and also the multi-photon absorption limit on the incident applied intensity, then the conversion efficiency is independent of the order of the nonlinear optical polarizability employed, and also of the oscillator strengths and positions of the intermediate levels. If intermediate levels have smaller oscillator strengths or resonant denominators, the incident applied field is allowed to increase to yield the same conversion efficiency. Calculations are performed for harmonic generation in Xe and  $\text{Li}^+$  and are shown in Table I. From this table we see that higher-order polarizations may equal or exceed lower order polarizations. The results of these calculations along with the analysis are published in Physical Review Letters, and is included as Appendix C of this report. Recently the fifth order processes  $5 \times 5320 \text{ \AA} \rightarrow 1064 \text{ \AA}$  and  $4 \times 5320 \text{ \AA} + 1.06\mu \rightarrow 1182 \text{ \AA}$  have been demonstrated experimentally in xenon. The experimental conversion efficiencies are low compared to theoretical predictions. However, for theory to hold, the media must be negatively dispersive and the applied power density must be approaching the multi-photon absorption or ionization limit. These

# CONVERSION EFFICIENCY AND LIMITING POWER DENSITY

Process	Specie	$(P/A)_{\text{max.}} (W/cm^2)$	Efficiency (Percent)
$3 \times 5320 \text{ \AA} \rightarrow 1773 \text{ \AA}$	Xe	$1.9 \times 10^{12}$	.08
$5 \times 5320 \text{ \AA} \rightarrow 1064 \text{ \AA}$	Xe	$1.9 \times 10^{12}$	.05
$5 \times 1192 \text{ \AA} \rightarrow 236 \text{ \AA}$	$Li^+$	$1.7 \times 10^{15}$	.002
$7 \times 1182 \text{ \AA} \rightarrow 169 \text{ \AA}$	$Li^+$	$1.7 \times 10^{15}$	.004
$15 \times 2660 \text{ \AA} \rightarrow 177 \text{ \AA}$	$Li^+$	$3.5 \times 10^{15}$	$4 \times 10^{-7}$

TABLE I--Limiting power density and conversion efficiency for some higher-order nonlinear process.



conditions may not be satisfied in those early experiments. More rigorous experiments including a better choice of the nonlinear media and addition of electrodes in the gas cell to determine degree of ionization will be conducted in the near future.

Based on the theory on higher-order polarizabilities, we have proposed a new experiment for generating radiation shorter than  $300 \text{ \AA}$ . The  $2p^5(^2P_{1/2}^0) 6s$  level of  $\text{Na}^+$  at  $274 \text{ \AA}$  is  $1.2 \text{ \AA}$  ( $1581 \text{ cm}^{-1}$ ) below the 39th harmonic of  $1.06 \mu$  at  $272.8 \text{ \AA}$ . Thus the fifth order process  $4 \times 1182 \text{ \AA} + 3547 \text{ \AA} \rightarrow 272.8 \text{ \AA}$  will be negatively dispersive. Estimates show that if the  $1182 \text{ \AA}$  radiation is focused to a density of  $1.2 \times 10^{14} \text{ W/cm}^2$ , then in one coherence length the conversion efficiency from  $3547 \text{ \AA}$  radiation to  $272.8 \text{ \AA}$  radiation will be  $2 \times 10^{-4}$ . Thus with  $10^8$  watts peak at  $1182 \text{ \AA}$  and a singly ionized sodium density of  $10^{17} \text{ ions/cm}^3$ ,  $10^8$  photons will be generated corresponding to a peak power of about  $150 \text{ W}$  at  $272.8 \text{ \AA}$ . Experimentally, ionization of sodium will be accomplished by the incident  $1182 \text{ \AA}$  laser pulse. At ion densities of  $10^{17} \text{ ions/cm}^3$ , recombination times are several nanoseconds and avalanche breakdown power densities are in excess of  $10^{15} \text{ W/cm}^2$ .

The uncertainties involved with this experiment include the validity of the higher-order polarizabilities theory, the coherence of the radiation generated by atoms spaced more than one wavelength apart, and the ability to maintain a column of singly ionized vapor. These problems will be studied during the coming quarter along with the construction of a miniature sodium heat-pipe oven and generation of high power  $1182 \text{ \AA}$  radiation in a mixture of xenon and argon.

Work on this project is jointly supported by the Office of Naval Research and the U.S. Air Force Cambridge Research Laboratories.

APPENDIX A

SECOND HARMONIC GENERATION AND INFRARED MIXING IN  $\text{AgGaSe}_2$

R.L. Byer, M.M. Choy, R.L. Herbst, D.S. Chemla\*  
and R.S. Feigelson<sup>†</sup>

Microwave Laboratory  
W.W. Hansen Laboratories of Physics  
Stanford University  
Stanford, California

\*Visiting from CNET, Bagneux, France

<sup>†</sup>Center for Materials Research, Stanford University

## SECOND HARMONIC GENERATION AND INFRARED MIXING IN $\text{AgGaSe}_2$

R.L. Byer, M.M. Choy, R.L. Herbst, D.S. Chemla\*  
and R.S. Feigelson

### ABSTRACT

We have continuously tuned between  $7\ \mu$  and  $15\ \mu$  by mixing the output of a  $\text{LiNbO}_3$  parametric oscillator in the chalcopyrite  $\text{AgGaSe}_2$ . We have doubled a  $\text{CO}_2$  laser with 2.7% efficiency which agrees very well with the expected efficiency and verifies the high optical quality of the 1.53 cm long  $\text{AgGaSe}_2$  crystal. The measured transparency range, indices of refraction, and nonlinear coefficient of  $d_{36} = 38 \times 10^{-12}$  m/V show that  $\text{AgGaSe}_2$  is a useful infrared nonlinear material phase-matchable over the entire  $3\ \mu$  to  $18\ \mu$  infrared region.

## SECOND HARMONIC GENERATION AND INFRARED MIXING IN $\text{AgGaSe}_2$

Since the first demonstration of phasematched second harmonic generation (SHG) in  $\text{AgGaSe}_2$ <sup>1</sup>, the nonlinear properties of the ternary semiconductors with chalcopyrite structure have been widely studied.<sup>2-6</sup> Their large nonlinear susceptibilities together with adequate birefringence to achieve phasematching make them attractive for nonlinear optical devices. Nonlinear mixing has been demonstrated in  $\text{ZnGeP}_2$ <sup>7</sup>,  $\text{AgGaSe}_2$ <sup>8,9</sup>,  $\text{CdGeAs}_2$ <sup>10,11</sup> and recently  $\text{AgGaSe}_2$ <sup>11,12</sup>

$\text{AgGaSe}_2$  single crystals are grown by the vertical Bridgman method after the starting materials are presynthesized in an amorphous carbon boat contained in a sealed quartz crucible. The presynthesized stoichiometric mix with a melting point of approximately  $860^\circ\text{C}$  is then transferred to a quartz crucible heavily coated with pyrolytic carbon for a pre-growth run at 2 mm per hour rate through a  $40^\circ\text{C}/\text{cm}$  temperature gradient. The top and bottom of the resulting boule are then removed prior to the actual growth run which takes place in the same vertical furnace but at a slower growth rate of 0.2 mm per hour. After growth the crucible is cooled to room temperature at  $25^\circ\text{C}$  per hour. The resulting 14 mm diameter single crystals typically show a gallium rich region near the seed end followed by approximately a 2 cm useful  $\text{AgGaSe}_2$  single crystal region and a silver rich top section. Early crystals showed a precipitate which resulted in a  $2\text{ cm}^{-1}$  scatter loss. In recent crystals the scatter loss has been significantly reduced with a corresponding reduction in loss to near  $.04\text{ cm}^{-1}$ . All crystals have high resistivity and good optical transparency from the bandgap at  $.71\text{ }\mu$  to the two phonon absorption edge at  $18\text{ }\mu$ . A particularly attractive feature of  $\text{AgGaSe}_2$  is the ease with which single crystals can be grown.



We have measured the nonlinear coefficient of  $\text{AgGaSe}_2$  relative to GaAs at  $10.6 \mu$ . Two methods used for relative nonlinear coefficient measurement are the Maker fringe method<sup>13</sup> and the wedge technique.<sup>14,15,6</sup> In both cases, the second harmonic power in the weak focusing low loss limit is given by<sup>16,17</sup>

$$P(2\omega) = K \left\{ \frac{d_{\text{eff}} t_2 t_1^2 E^2}{n_\omega^2 - n_{2\omega}^2} \right\}^2 \left\{ 1 - F \left( \frac{\pi \Lambda}{l_c(\theta)} \right) \cos \left( \frac{\pi l}{l_c(\theta)} \right) \right\} \quad (1)$$

where  $K$  is a constant,  $P(2\omega)$  is the second harmonic power,  $d_{\text{eff}}$  is the effective nonlinear coefficient,  $t_1$  and  $t_2$  are the crystal transmittances at the fundamental and harmonic,  $E$  is the fundamental field, and  $F(x) = \frac{2J_1(x)}{x}$  is a visibility factor with  $\Lambda = w_0 \tan \alpha$ , where  $w_0$  is the fundamental spot size. Here  $\alpha$  is the wedge apex angle and  $l$  the sample thickness and it is assumed that the fundamental beam is incident normal to the input face of the wedge. The Maker fringe method is useful for low index materials with large birefringence. The wedge method is suited for small birefringence large index materials. For the wedge method the coherence length is given by

$$l_c = \frac{\lambda}{4(n_{2\omega} - n_\omega)} = \frac{1}{2} \Delta y \tan \alpha \quad (2)$$

where  $\Delta y$  is the wedge translation distance between SHG extrema. For our crystal samples the coherence lengths are expected to be near  $100 \mu$  for GaAs and  $200 \mu$  for  $\text{AgGaSe}_2$  at  $10.6 \mu$

We used a (001) oriented  $\text{AgGaSe}_2$  wedge for the nonlinear susceptibility measurement relative to two GaAs reference samples. GaAs material supplied by Coherent Radiation Laboratories was cut in a (001) direction, and (111) oriented wedge was cut from Monsanto material. Both GaAs samples were

chromium compensated to a high resistivity of about  $10^7 \Omega \text{ cm}$ . With the laser polarization parallel to the (110) direction,  $E_x = E_y = E_o/\sqrt{2}$  and  $P = P_z = d_{36} E_o^2$  so the  $d_{\text{eff}}$  for the (001) cut  $\text{AgGaSe}_2$  and GaAs samples are  $d_{36}$  and  $d_{36} = d_{14}$  respectively. For the (111) cut GaAs, with the laser polarization along (111) direction,  $E_x = E_y = E_z = E_o/\sqrt{3}$ , and so  $P = 2/\sqrt{3} d_{14} E_o^2$  and the  $d_{\text{eff}}$  in this case is  $2/\sqrt{3} d_{14}$ . A summary of the parameters are given in Table I. The coherence length of GaAs is measured to be  $107 \pm 2 \mu\text{m}$  and  $109 \pm 3 \mu\text{m}$  for the (001) and (111) cut samples. This is in excellent agreement with published values in references 18 and 19 of  $107 \pm 5 \mu\text{m}$  and  $107 \pm 1 \mu\text{m}$ . The measured coherence length of  $\text{AgGaSe}_2$  is  $237 \pm 15 \mu\text{m}$ . This compares favorably with a calculated value of  $255 \pm 50 \mu\text{m}$ , based on Boyd et al.,<sup>6</sup> index data with an assumed accuracy of the third decimal place in the index. For the analysis we used an extension of Eq. (1) given in reference 19 which includes a factor due to crystal loss. The  $\text{AgGaSe}_2$  nonlinear coefficient measured relative to GaAs is

$$R_{001} = \frac{d_{36}(\text{AgGaSe}_2)}{d_{14}(\text{GaAs})} = 0.33 \pm 25\%$$

and

$$R_{111} = \frac{d_{36}(\text{AgGaSe}_2)}{d_{14}(\text{GaAs})} = 0.32 \pm 18\%$$

These values are in good agreement with Boyd et al's.,<sup>6</sup> value of  $0.37 \pm 10\%$  and with Kildal's recent measurement.<sup>11</sup> With  $d_{14}(\text{GaAs}) = 117 \times 10^{-12} \text{ m/V}$ <sup>20</sup> and using the average of the two ratios we obtain  $d_{36}(\text{AgGaSe}_2) = 38 \times 10^{-12} \text{ m/V}$ .

TABLE I

Measurement of  $\text{AgGaSe}_2$  SHG Nonlinear Coefficient

	GaAs	GaAs	$\text{AgGaSe}_2$
Crystal Orientation	(001)	(111)	(001)
Wedge Angle	$11^\circ 13'$	$16^\circ 2'$	$15^\circ 53'$
$d_{\text{eff}}$	$d_{14}$	$2/\sqrt{3} d_{14}$	$d_{36}$
$\alpha_1$	$0.2 \text{ cm}^{-1}$	$0.2 \text{ cm}^{-1}$	$2 \text{ cm}^{-1}$
$\alpha_2$	$0.3 \text{ cm}^{-1}$	$0.3 \text{ cm}^{-1}$	$3 \text{ cm}^{-1}$
$l_c$ ( $\mu\text{m}$ ) measured	$107 \pm 2$	$109 \pm 3$	$237 \pm 15$
$R \equiv \frac{d_{36}(\text{AgGaSe}_2)}{d_{14}(\text{GaAs})}$	1	1	$0.33 \pm 25\%$ $0.32 \pm 18\%$

We have also performed phasematched SHG of  $10.6 \mu$  using a  $60^\circ$  cut  $\text{AgGaSe}_2$  crystal. The measured phasematching angle of  $57.5^\circ \pm .5^\circ$  is in good agreement with the calculated value of  $55^\circ \pm 4^\circ$ . The expected phase-matched SHG conversion efficiency is

$$\frac{P_{2\omega}}{P_{\omega}} = \Gamma^2 \ell^2 = \left( \frac{2\omega^2 d_{\text{eff}}^2}{\pi n_{\omega}^2 n_{2\omega} \epsilon_0 c^3} \right) P_{\omega} \ell k_{\omega} h(B, \xi) \quad (3)$$

where the powers are defined inside the crystal,  $d_{\text{eff}} = d_{36} \sin \theta_m$ ,  $\ell$  is the crystal length,  $k = 2\pi n_{\omega}/\lambda$ , and  $h(B, \xi)$  is the Boyd and Kleinman<sup>21</sup> focusing factor which reduces to  $\ell/b = \ell/w_0^2 k$  in the loose focusing limit. For a low loss  $\text{AgGaSe}_2$  crystal 1 cm in length in the loose focusing limit ( $\ell/b < 1$ ) the calculated SHG conversion efficiency is  $\Gamma^2 \ell^2 = 0.75\%$  at  $1 \text{ MW/cm}^2$ . Using a TEA  $\text{CO}_2$  laser operating in a  $\text{TEM}_{00}$  mode as a source, we measured the absolute SHG efficiency generated in a high quality 1.54 cm long  $\text{AgGaSe}_2$  crystal. The average input and output powers measured with an Eppley thermopile were 2.82 mW and  $76 \mu\text{W}$ , which corresponds to 1.6 kW and 44 W of peak power at the fundamental and second harmonic. The experimentally observed conversion efficiency for the incident intensity of  $1.68 \text{ MW/cm}^2$  is 2.68%. Using  $d_{36} = 38 \times 10^{-12} \text{ m/V}$ ,  $\ell = 1.54 \text{ cm}$  and  $h(B, \xi) = .925 \ell/b$  which corresponds to the focal spot size of  $250 \mu$ , the expected conversion efficiency is 2.76%. This measurement can be considered as a separate absolute determination of the nonlinear coefficient of  $\text{AgGaSe}_2$ . The nonlinear coefficient is found to be

$$d_{36} = 40 \pm 1 \times 10^{-12} \frac{\text{m}}{\text{V}}$$

which agrees very well with the previous measurement made relative to GaAs.

AgGaSe<sub>2</sub> phasematches for SHG for fundamental wavelengths between 3 μ and 13 μ. The SHG efficiency of AgGaSe<sub>2</sub> is significantly better than proustite, for example, due to both a factor of three increase in the nonlinear coefficient and the small birefringence which allows increased interaction lengths without aperture length limitations.

AgGaSe<sub>2</sub> has adequate birefringence to phasematch over an extended infrared spectral range for tunable wavelength generation by mixing. For mixing a convenient tunable pump source is a LiNbO<sub>3</sub> parametric oscillator<sup>22</sup> mixing against fixed frequency Nd:YAG laser. For our experiment we used a collinear geometry. The acoustic Q-switched Nd:YAG laser tuned to 1.32 μ is internally doubled with a LiIO<sub>3</sub> crystal to generate 0.659 μ which pumps the temperature tuned LiNbO<sub>3</sub> oscillator. The oscillator output in the 1.5 - 1.7 μ range mixes with the remaining collinear 1.32 μ beam in the AgGaSe<sub>2</sub> crystal. The AgGaSe<sub>2</sub> is angle phasematched by rotation on a geared stage.

The mixing efficiency is given by

$$\frac{P_{IR}}{P_{osc}} = \left( \frac{\omega_{IR}^2 d_{eff}^2 \ell^2}{n_p n_{osc} n_{IR} c^3 \epsilon_0} \right) \frac{P_p}{A} \text{sinc}^2 \left( \frac{\Delta k \ell}{2} \right) \quad (4)$$

where the pump wavelength is 1.32 μ,  $A = \pi/2 (\omega_{osc}^2 + \omega_p^2)$  and  $\theta_m$  is the phasematching angle. For a 1 cm AgGaSe<sub>2</sub> crystal at a pump intensity of 1 MW/cm<sup>2</sup> at 1.32 μ, the conversion efficiency is  $P_{IR}/P_{osc} = 1.2\% (\omega_{IR}/\omega_{osc})$ .

Figure 1 shows the generated mixed output from 7 μ to 15 μ. Beyond 15 μ our HgCdTe detector is response limited. Figure 2 shows the phasematching peak generated by mixing in a fixed AgGaSe<sub>2</sub> crystal by a tunable LiNbO<sub>3</sub>



oscillator pump. The characteristic  $\text{sinc}^2 \left( \frac{\Delta k \ell}{2} \right)$  phasematching peak-width agrees with that calculated from the dispersion of  $\text{AgGaSe}_2$ .

A plot of the phasematching angle vs  $\text{LiNbO}_3$  oven temperature showed a nearly linear relation over a wide  $7 \mu$  to  $12 \mu$  spectral range. We therefore used a stepping motor and synchronously rotated the  $\text{AgGaSe}_2$  crystal to phasematch with a  $1^\circ\text{C}$  per minute temperature scanned  $\text{LiNbO}_3$  parametric oscillator. In this way the spectrum between  $7 \mu$  and  $12 \mu$  was continuously tuned in eight minutes. The output bandwidth of this coherent source is  $2 \text{ cm}^{-1}$  which is determined by the parametric oscillator's  $2 \text{ cm}^{-1}$  gain bandwidth.

Figure 3 shows a spectrum of polystyrene as an example of the continuous scanning capability of this source. The spectrum was taken using a dual channel differential boxcar with two  $\text{HgCdTe}$  detectors. The mixed output is detected with better than a 30 db signal to noise ratio with a peak to peak variation of less than 10% at a repetition rate between 10 - 25 pps.

When mixing against  $1.32 \mu$ ,  $\text{AgGaSe}_2$  does not have adequate birefringence to phasematch at wavelengths shorter than  $7 \mu$ . Based on phasematching calculations with the aid of Boyd et al's.,<sup>6</sup> index of refraction data, mixing against wavelengths  $1.5 \mu$  and longer allow complete coverage of the infrared. As an example, a  $1.06 \mu$  pumped  $\text{LiNbO}_3$  parametric oscillator with degeneracy near  $2.12 \mu$  angle tunes over a  $1.5 \mu$  to  $3.7 \mu$  range.  $\text{AgGaSe}_2$  phasematches for mixing the signal and idler waves to generate  $3 \mu$  to  $18 \mu$  for phasematching angles between  $80^\circ$  and  $50^\circ$ .<sup>12</sup> This example shows the unique phasematching properties of  $\text{AgGaSe}_2$  for extended infrared generation by mixing.

In conclusion, we have measured the nonlinear coefficient of  $\text{AgGaSe}_2$  and demonstrated phasematched SHG of a  $\text{CO}_2$  laser as a verification of crystal quality and potential use as a second harmonic generator. Using a  $\text{LiNbO}_3$  parametric oscillator as source, we have generated continuously tunable output between  $7\ \mu$  and  $15\ \mu$  by mixing in  $\text{AgGaSe}_2$ . This experiment demonstrates the useful phasematching and nonlinear properties of  $\text{AgGaSe}_2$  for infrared generation.

#### ACKNOWLEDGEMENT

We wish to acknowledge the assistance of Dr. R. Route and R. Raymaker for growth of the  $\text{AgGaSe}_2$  crystals.

This research was supported in part by the Advance Research Projects Agency of the Department of Defense and monitored by the Air Force Materials Laboratory, LP under Contract F33615-72-C-2001, in part by the U.S. Army Research Office, Durham, under Contract DA-ARO-D-31-124-72-G-184 and in part by Honeywell Research Laboratories.

## REFERENCES

1. D.S. Chemla, P.J. Kupeck, D.S. Robertson, R.C. Smith, "Silver Thiogallate a New Material with Potential for Infrared Devices", Optics. Comm. 3, 29, (1971).
2. G.D. Boyd, E. Beuhler, F.G. Storz, J.H. Wernick, "Linear and Non-linear Optical Properties of  $\text{ZnGeP}_2$  and  $\text{CdSe}$ ", Appl. Phys. Letts. 18, 301, (1971).
3. R.L. Byer, H. Kildal, R.S. Feigelson, " $\text{CdGeAs}_2$  a New Nonlinear Crystal Phase Matchable  $10.6 \mu\text{m}$ ", Appl. Phys. Letts. 19, 237, (1971).
4. G.D. Boyd, H. Kasper, J.H. McFee, "Linear and Nonlinear Optical Properties of  $\text{AgGaSe}_2$ ,  $\text{CuGaS}_2$ , and  $\text{CuInS}_2$  and Theory of the Wedge Technique for the Measurement of Nonlinear Coefficients", IEEE, QE-7, 563, (1971).
5. G.D. Boyd, E. Buehler, F.G. Storz, J.H. Wernick, "Linear and Non-linear Optical Properties of Ternary  $\text{A}^{\text{II}} \text{B}^{\text{IV}} \text{C}_2^{\text{V}}$  Chalcopyrite Semiconductors", IEEE, QE-8, 419, (1972).
6. G.D. Boyd, H. Kasper, J.H. McFee, F.G. Storz, "Linear and Nonlinear Optical Properties of Some Ternary Selenides", IEEE, QE-8, 900, (1972).
7. G.D. Boyd, T.J. Bridges, C.K.N. Patel, E. Buehler, "Phase Matched Submillimeter Wave Generation by Difference Frequency Mixing in  $\text{ZnGeP}_2$ ", Appl. Phys. Letts. 21, 553, (1972).
8. C.G. Bethea, "Megawatt power at  $1.318 \mu\text{m}$  in  $\text{Nd}^{3+}$ :YAG and Simultaneous Oscillation both at  $1.06$  and  $1.318 \mu\text{m}$ ", IEEE, QE-9, 254, (1973).

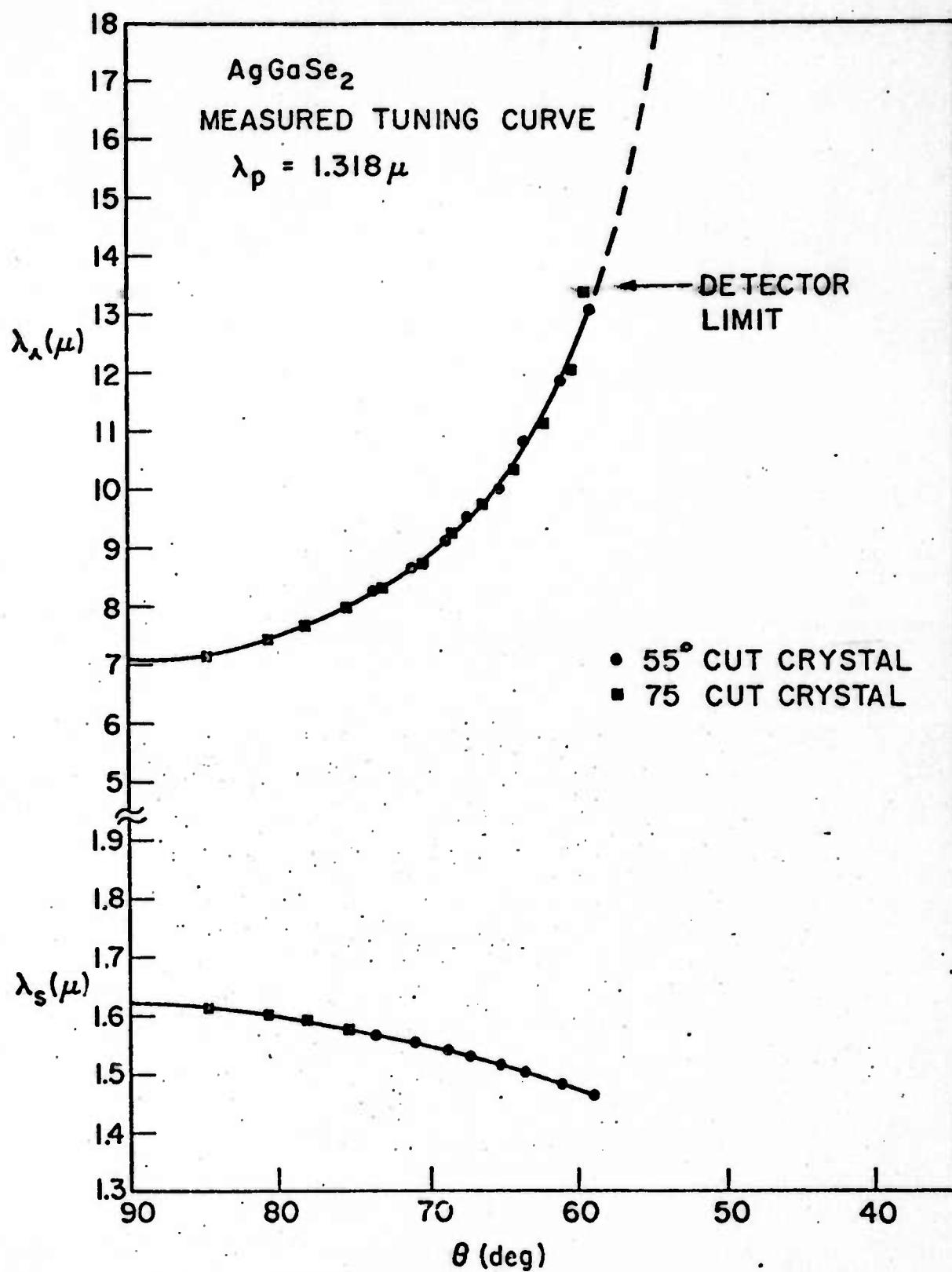
9. D.C. Hanna, V.V. Rappal and R.C. Smith, "Tunable Infrared Down-Conversion in Silver Thiogallate", Optics Communications, Vol. 8, p.151, (1973).
10. H Kildal, R.F. Begley, M.M. Choy and R.L. Byer, "Efficient Second and Third Harmonic Generation in  $\text{CdGeAs}_2$ ", JOSA 62, p.1398, (1972).
11. H. Kildal, Conference on Laser Applications, Washington. D.C. (1973).
12. R.L. Byer, M.M. Choy and R.L. Herbst, Conference on Laser Applications, Washington. D.C. (1973), see also R.L. Byer, "Parametric Oscillators", Proc. of First Tunable Laser Spectroscopy Conference, Vail, Colorado, June 1973, (to be published).
13. P.D. Maker, R.W. Terhune, N. Nisenhoff and C.M. Savage, "Effects of Dispersion and Focusing on the Production of Optical Harmonics", Phys. Rev. Letts. Vol. 8, p.21. (1962).
14. J. Jerphagnon, Ph.D. Thesis, University of Paris, (1966).
15. J.J. Wynne and N. Bloembergen, "Measurement of the Lowest Order Non-linear Susceptibility in III - V Semiconductors by Second Harmonic Generation with a  $\text{CO}_2$  Laser", Phys. Rev. 188, p.1211, (1969).
16. D.S. Chemla, P. Kupecek, "Analyse des Experiences de Generation de Second Harmonique", Rev. Phys. Appl. 6, p.31, (March 1971).
17. D.S. Chemla, Ph.D. Thesis, University of Paris, (1972), Ann. Telecom. 27, N7-8, p.311, (1972).

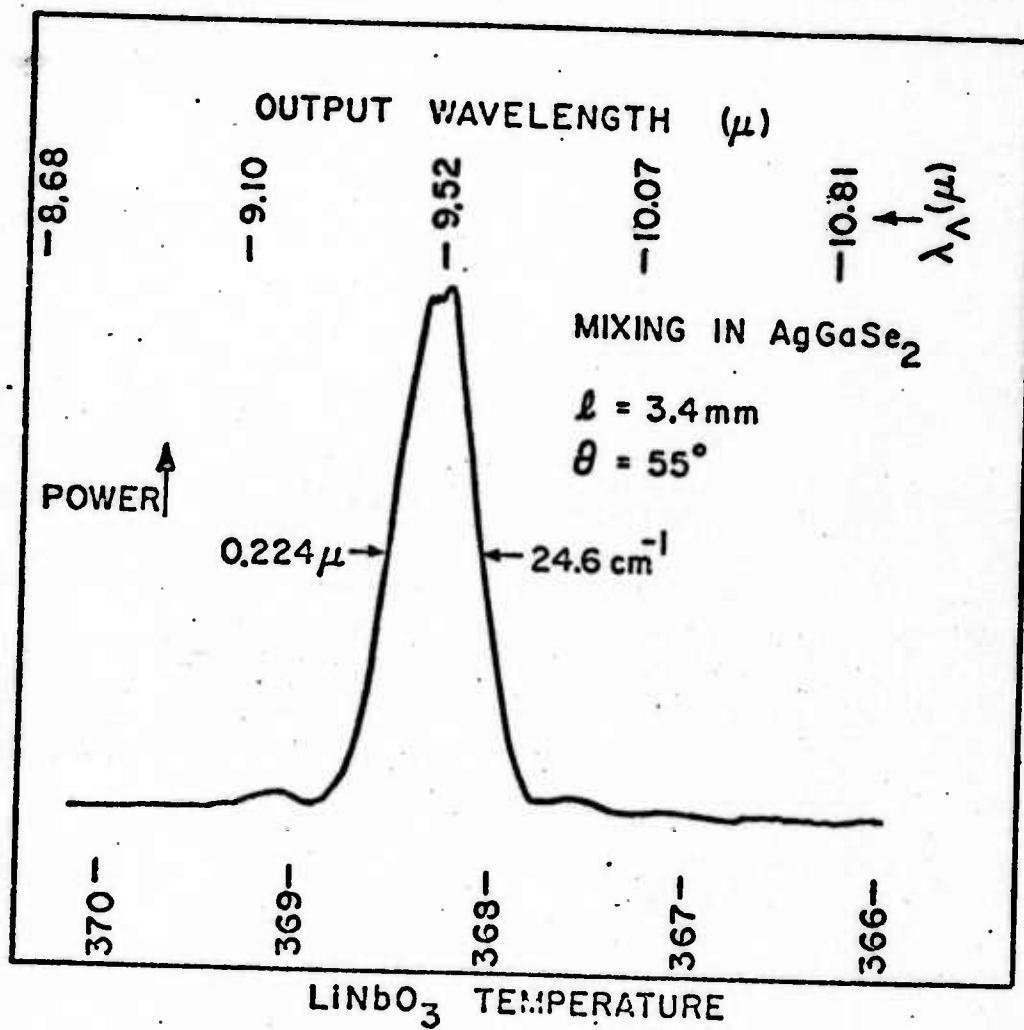
18. J.H. McFee, G.D. Boyd and P.H. Schmidt, "Redetermination of the Nonlinear Optical Coefficients of Te and GaAs by Comparison to  $\text{Ag}_3\text{SbS}_3$ ", Appl. Phys. Letts. 17, p.57, (1970).
19. D.S. Chemla, P.J. Kupecek and C.A. Schwartz, "Redetermination of the Nonlinear Optical Coefficients of Proustite by Comparison with Pyrargyrite and Gallium Arsenide", Opt. Comm. Vol. 7, p.225, (1973).
20. D.S. Chemla, R.F. Begley, R.L. Byer, "Experimental and Theoretical Studies of Third Harmonic Generation in the Chalcopyrite  $\text{CdGeAs}_2$ ", (to be published).
21. G.D. Boyd, D.A. Kleinman, "Parametric Interaction of Focused Gaussian Light Beams", J. Appl. Phys. 39, p.3597, (1968).
22. R.W. Wallace, "Stable, Efficient, Optical Parametric Oscillators Pumped with Doubled Nd:YAG", Appl. Phys. Letts. 17, p.497, (1970).

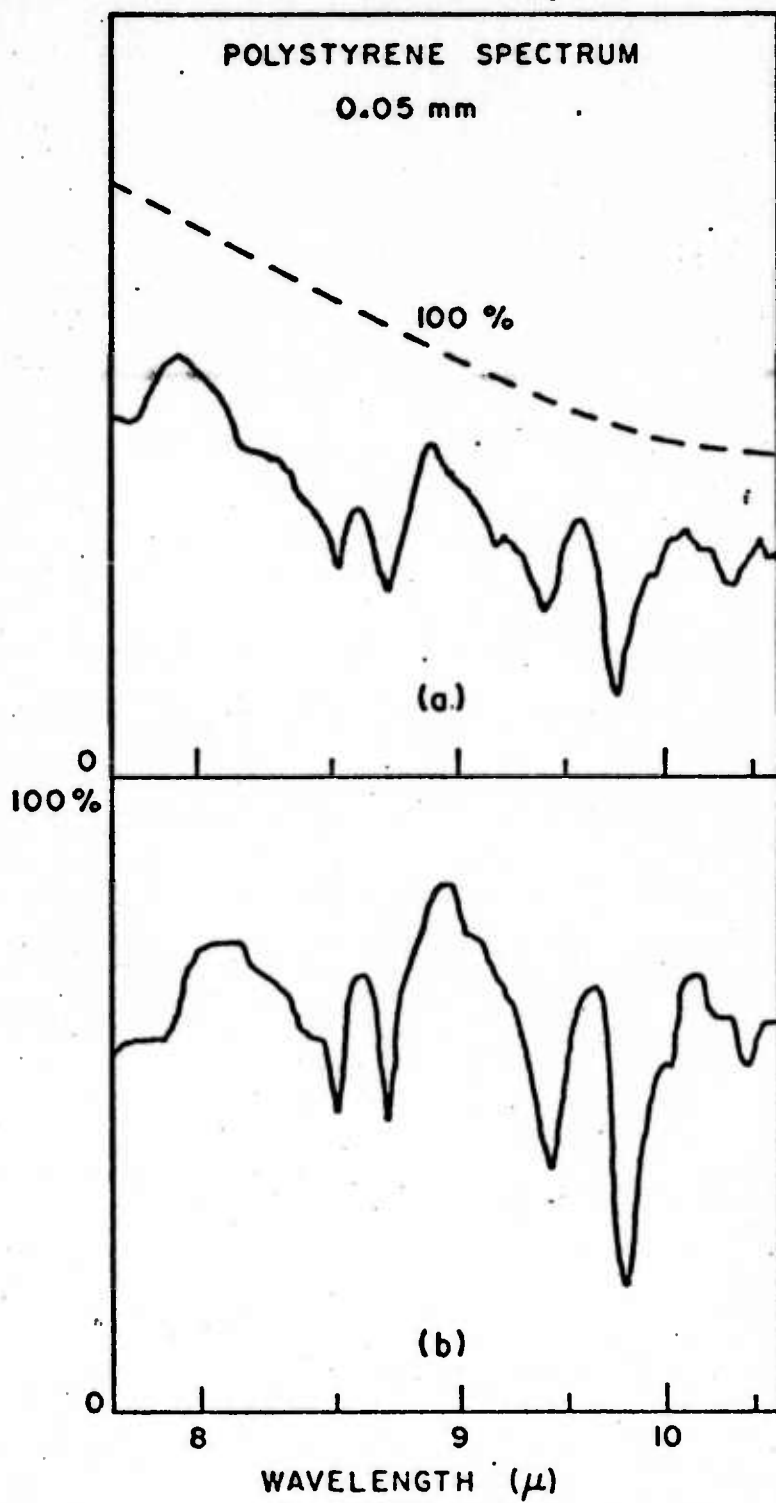


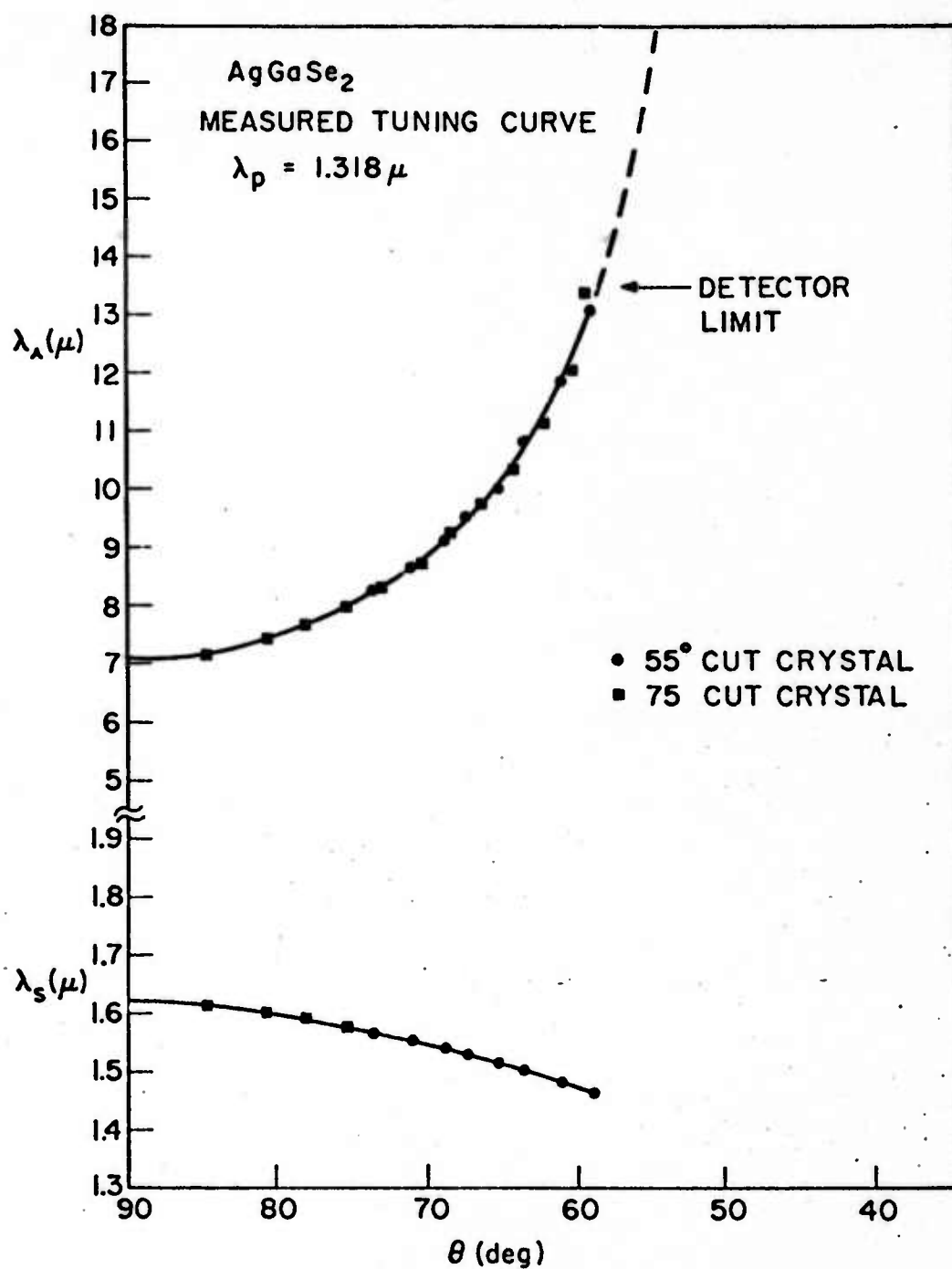
#### FIGURE CAPTIONS

1. The  $7\ \mu$  to  $15\ \mu$  mixing output in angle phasematched  $\text{AgGaSe}_2$  pumped by a  $1.318\ \mu$  Nd:YAG laser mixing with a  $.659\ \mu$  pumped  $\text{LiNbO}_3$  parametric oscillator.
2. Phasematched mixing peak generated in  $\text{AgGaSe}_2$  held at a fixed angle.
3. The spectrum of polystyrene taken with the  $\text{AgGaSe}_2$  mixer (top) and Perkin Elmer Spectrophotometer (bottom).

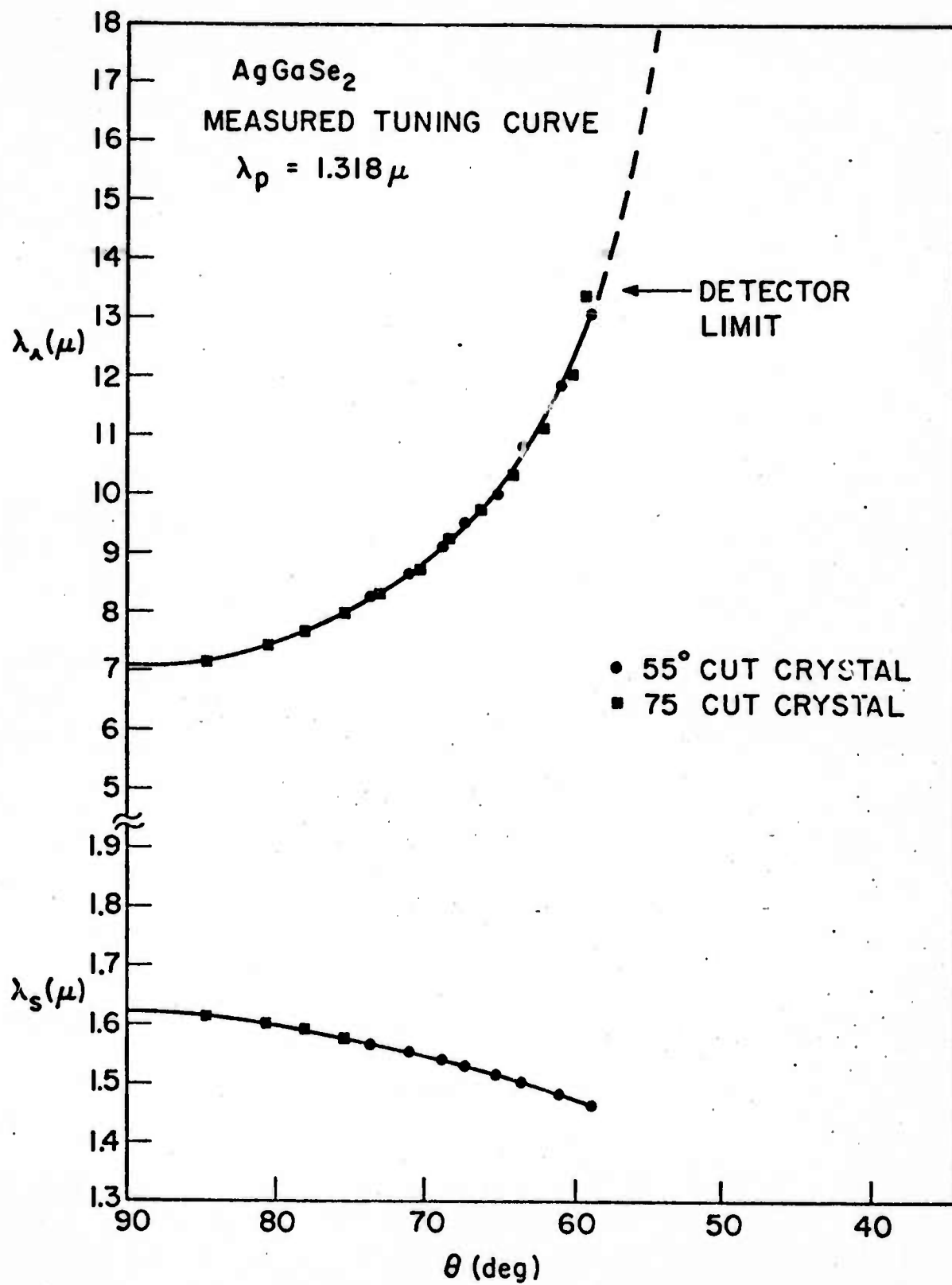












APPENDIX B

PARAMETRIC OSCILLATORS

by

Robert L. Byer

for

Laser Spectroscopy Conference  
Vale, Colorado, June 1973

Microwave Laboratory  
W.W. Hansen Laboratories of Physics  
Stanford University  
Stanford, California

## PARAMETRIC OSCILLATORS

### I. INTRODUCTION

Parametric oscillators and parametric mixing and sum generation devices offer the widest tuning range of known coherent sources. This paper reviews the present state of parametric devices with a bias toward their use in spectroscopy. In addition to tuning range, bandwidth and bandwidth narrowing methods are considered. The discussion includes the properties of new infrared nonlinear materials that permit parametric tuning over the entire infrared spectrum. Finally, application of parametric oscillators to spectroscopy is illustrated and predictions of future tuning range and output performance is discussed.

$\text{LiNbO}_3$  optical parametric oscillators are now in wide use. The properties of parametric oscillators have been reviewed by Harris<sup>1</sup> and recently by Smith<sup>2</sup> and Byer.<sup>3</sup> Parametric oscillator sources cover a spectral range from  $0.4 \mu$  to  $0.8 \mu$  with ADP<sup>4</sup>,  $0.6 \mu$  to  $3.5 \mu$  with  $\text{LiNbO}_3$ <sup>5</sup>,  $2 \mu$  and  $9.6 \mu$  to  $11 \mu$  in CdSe<sup>6</sup> and  $1.22 \mu$  to  $8.5 \mu$  with proustite.<sup>7</sup>  $\text{LiNbO}_3$  is the best developed parametric oscillator and is the only oscillator available commercially.

If we include mixing and sum generation in our general definition of parametric sources, then these three frequency processes satisfy the energy and momentum conservation conditions

$$\omega_3 = \omega_2 + \omega_1 \quad (1)$$

$$k_3 = k_2 + k_1 \quad (2)$$

The interaction takes place in the nonlinear material with a gain or conversion efficiency given by

$$G = \Gamma^2 \ell^2 = \left( \frac{2 \omega_o^2 d^2}{\pi n_o^2 n_3 \epsilon_o c^3} \right) P_{30} \ell k_o (1 - \delta^2)^2 \bar{h}(B, \xi) \quad (3)$$

where  $\omega_o$  is the degenerate angular frequency,  $d$  is the nonlinear coefficient in mks units

$$d \left( \frac{m}{V} \right) = \left( \frac{3 \times 10^4}{4 \pi} \right) d \text{ (cm/statvolt)}$$

$P_{30}$  is the pump power,  $\ell$  the crystal length,

$$k_o = \frac{2\pi n_o}{\lambda_o} \quad (4)$$

and

$$(1 - \delta^2) = \omega_1 \omega_2 / \omega_o^2 \quad (5)$$

is the degeneracy factor, and  $\bar{h}(B, \xi)$  is the Boyd and Kleinman<sup>9</sup> focusing factor.

For parametric oscillators and mixing experiments, the gain reduces to

$$G(\ell) = \Gamma^2 \ell^2 \text{sinc}^2 \left( \frac{\Delta k \ell}{2} \right) \quad (6)$$

in the low gain limit and to

$$G(\ell) = \frac{1}{4} \exp 2\Gamma \ell \quad (7)$$

in the high gain limit. Here  $\text{sinc}^2(\Delta k \ell / 2)$  is the phase mismatch factor which leads to an expression for the bandwidth of the interaction. For sum generation the conversion efficiency is the same in the low conversion limit but varies as  $\sin^2 \Gamma \ell$  in the high conversion limit.

Equation (3) shows that focusing determines the mixing conversion efficiency and parametric gain through the focusing parameter  $\bar{h}(B, \xi)$  which describes coupling between gaussian modes as a function of the double refraction parameter

$$B = \frac{1}{2} \rho (\ell k_0)^{\frac{1}{2}} \quad (8)$$

and the focusing parameter

$$\xi = \ell / b \quad (9)$$

where the confocal parameter

$$b = W_0^2 k_0 = \frac{W_0^2 2\pi n_0}{\lambda_0} \quad (10)$$

Here  $W_0$  is the gaussian beam electric field radius such that the power in the gaussian beam is related to the peak intensity by

$$P = I_0 (\pi W_0^2 / 2) \quad (11)$$

The double refraction parameter is a function of the double refraction



angle  $\rho$  given by

$$\tan \rho = \frac{n_o^2}{2} \left[ \frac{1}{n^e(\theta)^2} - \frac{1}{(n_o^o)^2} \right] \sin 2\theta \quad (12)$$

where  $\theta$  is the propagation direction with respect to the optic axis and we have assumed  $n^e < n^o$  or a negative uniaxial crystal.

In terms of the aperture length

$$l_a = \frac{W_o \sqrt{\pi}}{\rho} \quad (13)$$

the double refraction parameter can be written as

$$B = \frac{\sqrt{\pi}}{2} l/l_a \xi^{-\frac{1}{2}} \quad (14)$$

For parametric interactions  $\bar{h}(B, \xi)$  can usually be approximated by one of its limiting forms. In the near field approximation with negligible double refraction

$$\bar{h}(B, \xi) \rightarrow \xi \cdot \left( \xi < 0.4, \xi < \frac{1}{6B^2} \right) \quad (15)$$

For confocal focusing where  $\xi = 1$

$$\bar{h}(0, 1) \rightarrow 1 \quad (16)$$

which corresponds to the near field focusing limit first discussed by Boyd and Ashkin<sup>10</sup>. In fact, the maximum value of  $\bar{h}(B, \xi) = \bar{h}_{mm}(0, 2.84) = 1.068$  for  $\xi = 2.84$  instead of  $\xi = 1$ . However, practical considerations usually limit focusing such that  $\xi < 1$ .

When double refraction is important the gain reduction factor is closely approximated by the expression<sup>9</sup>

$$\bar{h}_{mm}(B) \approx \frac{1}{1 + (4B^2/\pi)} \quad (17)$$

which can be rewritten as

$$\bar{h}_{mm}(B) \approx \frac{1}{1 + (\ell/\ell_{eff})} \quad (18)$$

where the effective interaction length is given by

$$\ell_{eff} = \frac{\lambda_o}{2 n_o \rho} \quad (19)$$

In the limit of strong double refraction where  $\ell/\ell_{eff} > 1$  the focusing parameter becomes

$$\bar{h}_{mm}(B) \rightarrow \ell_{eff}/\ell \quad (B^2/4 > \xi > 2/B^2) \quad (20)$$

so that the conversion efficiency as a function of input power is independent of crystal length. In addition, large double refraction maintains  $\bar{h}_{mm}(B)$  constant over a wide range of  $\xi$ . Thus to minimize crystal damage problems  $\xi$  can be chosen at the least value consistent with maximum  $\bar{h}_{mm}(B)$ . This value is given by

$$\xi > 2/B^2 \quad (21)$$

which yields a corresponding focal spot size

$$w_o \approx \frac{1}{2\sqrt{2}} \rho \ell \quad (22)$$

and corresponding area

$$\pi W_0^2/2 \lesssim \frac{\pi}{16} \rho^2 \ell^2 \quad (23)$$

Double refraction due to non-collinear phasematching results in a serious reduction of  $\Gamma^2 \ell^2$  for power limited pump conditions. For example, for  $\text{LiNbO}_3$  at room temperature, phasematched at  $\theta = 43^\circ$  for a  $1.06 \mu\text{m}$  pump source,  $\rho = 0.037$  radians and  $B = 4.7 \ell^{\frac{1}{2}}$ . The gain is reduced by  $\pi/4B^2 = \ell/\ell_{\text{eff}}$  which in this case is 28 times for a 1 cm crystal and 140 times for a 5 cm crystal compared to the  $90^\circ$  phasematched case. For this case  $\ell_{\text{eff}}$  is only .36 mm and  $\xi$  can vary between  $5.5 > \xi > 0.09$  without affecting the gain. This corresponds to a confocal parameter variation between 11 cm and .2 cm. For experimental ease and minimum incident intensity at the  $\text{LiNbO}_3$  crystal the 11 cm confocal focusing would be used. The pump intensity varies as  $\ell^2$  in agreement with Eq. (23).

For high power pumping conditions where more than adequate pump power is available, the minimum focal area may be dictated by the crystal damage intensity. Most semiconductor materials show surface damage at near  $1\text{J}/\text{cm}^2$ . For other nonlinear materials this energy density may approach  $4\text{J}/\text{cm}^2$ .<sup>11</sup> For focusing determined by incident pump energy density with areas larger than that given in Eq. (23), the double refraction gain reduction is correspondingly smaller. In this case,  $90^\circ$  phasematching maintains only the advantages of larger pump acceptance angle and larger effective nonlinear coefficient.

Table I lists selected nonlinear materials and their properties of interest in parametric interactions. Of particular interest for infrared generation is  $\text{LiNbO}_3$  proustite,  $\text{CdSe}$  and the four chalcopyrite crystals  $\text{AgGaS}_2$ ,  $\text{AgGaSe}_2$ ,  $\text{ZnGeP}_2$  and  $\text{CdGeAs}_2$ . The characteristics of tunable sources based on these materials are considered in detail by Byer.<sup>3</sup>

TABLE I  
Nonlinear Coefficient, Figure of Merit, and  
Gain for Nonlinear Crystals

MATERIAL (point group pump wavelength)	$d \times 10^{12}$ (m/V)	$n_o$ $n_e$	$n_o - n_e$	$\theta_m$	$\rho$	$d_{eff,12}$ $\times 10$	$d_{eff}^2/n_o^2 n_e^3$ $\times 10^{24}$	$\ell(p)_{eff}$ (cm)	$\Gamma^2 \ell^2$ 1 Watt	$\Gamma^2 \ell^2$ 1 W/cm <sup>2</sup>	$I_{burn}$ (W/cm <sup>2</sup> )	Transmission Range ( $\mu m$ )
CdGeAs <sub>2</sub> ( $\bar{4}2m$ ) $\lambda_p = 5.3 \mu m$	$d_{36} = 236^{b,c}$	3.51	+ .006	II 55°	.021	193 (d sin $\theta$ )	861	.34	$3.8 \times 10^{-4}$	.033	20 - 40	2.4 - 17
		3.59		I 35°	.021	212 (d sin $2\theta$ )	1039		$4.6 \times 10^{-4}$	.040		
ZnGeP <sub>2</sub> ( $\bar{4}2m$ ) $\lambda_p = 1.83 \mu m$	$d_{36} = 75^\circ$	3.11	+ .038	II 90°	0.0	$d_{36}$	187	$\ell = 1$ cm	$7.1 \times 10^{-3}$	.21	> 4	.7 - 12
		3.15		I 62°	0.01	62.2 (d sin $2\theta$ )	127	.59	$1.8 \times 10^{-3}$	.05		
AgGaSe <sub>2</sub> ( $\bar{4}2m$ ) $\lambda_p = 1.83 \mu m$	$d_{36} = 33^\circ$	2.62	-0.32	I 55°	.01	27 (d sin $\theta$ )	42	.71	$5.52 \times 10^{-4}$	.02	> 10	.73 - 17
		2.58		I 90°	0.0	$d_{36}$	63.4	$\ell = 1$ cm	$1.98 \times 10^{-3}$	.07		
CdSe (6 mm) $\lambda_p = 1.83 \mu m$	$d_{31} = 9^\circ, h$	2.45	+ .019	90°	0.0	$d_{31}$	24	$\ell = 2$ cm	$1.3 \times 10^{-3}$	.09	60	.75 - 25
		2.47										
AgGaSe <sub>2</sub> ( $\bar{4}2m$ ) $\lambda_p = .946 \mu m$	$d_{36} = 12^\circ$	2.42	- .094	I 64°	0.17	10.8 (d sin $\theta$ )	9.2	.14	$2.3 \times 10^{-4}$	.013	12 - 25	.60 - .33
		2.36		I 90°	0.0	$d_{36}$	11	$\ell = 1$ cm	$2.3 \times 10^{-3}$	.045		



Table I continued

MATERIAL (point group pump wavelength)	$d \times 10^{12}$ (m/V)	$n_o$ $n_{ce}$	$n_o - n_{ce}$	$\theta_m$	$\rho$	$d_{eff,12}$ $\times 10$	$d_{eff}^2/n_o^2 \times 10^{24}$	$r(\theta)_{eff}$ (cm)	$r^2 \ell^2$ 1 Watt	$r^2 \ell^2$ 1 MW/cm <sup>2</sup>	$I_{burn}$ (MW/cm <sup>2</sup> )	Transmission Range ( $\mu m$ )
$Fe_3AsS_3$ (3m) $\lambda_p = 1.06 \mu m$	$d_+ = 11.6^f$	2.76 2.54	-.223	30°	0.078	$d_+$	8.2	.007	$9.0 \times 10^{-6}$	.011	12 - 40	.60 - 13
$LiNbO_3$ (3m) $\lambda_p = .532$	$d_{31} = 6.25^k$	2.24 2.16	-.081	90°	0.0	$d_{31}$	3.88	$\ell = 5$ cm	$2.1 \times 10^{-2}$	1.28	50 - 140	.35 - 4.5
ADP (42m) $\lambda_p = .266$	$d_{36} = .57^{f,m}$	1.33 1.48	-.0458	90°	0.0	$d_{36}$	.100	$\ell = 5$ cm	$2.9 \times 10^{-3}$	.131	> 1000	.20 - 1.1

## References to Table I

- b) Dyer et al (1971)  
 c) Boyd et al (1972a)  
 e) Boyd et al (1971a)  
 f) Feichtner and Roland (1972)  
 g) Boyd et al (1971c)  
 h) Herbst and Dyer (1971)  
 i) Boyd et al (1971e)  
 k) Dyer and Harris (1968)  
 m) Bjorkholm and Siegman (1967)  
 L) Francois (1966)

## II. EXTENDED INFRARED TUNING

Of particular interest to spectroscopists is the extended tuning range available from parametric devices. In addition, bandwidth and techniques for bandwidth narrowing and ultimately single frequency operation are important.

There has been considerable progress recently in extending the tuning range of parametric oscillators. However, to date the most reliable parametric oscillator uses  $\text{LiNbO}_3$  at  $90^\circ$  phasematching with temperature tuning. This source covers with good efficiency and operating stability the spectral region from  $0.6 \mu$  to  $3.5 \mu$  with the second harmonic of a Q-switched Nd:YAG laser pump source operating at  $.532 \mu$ ,  $.561 \mu$  and  $.659 \mu$ . Figure 1 shows the experimental tuning curve for the  $.695 \mu$  pump wavelength. Also shown are the wavelengths generated by internal SHG and sum generation using  $\text{LiIO}_3$ . This singly resonant oscillator typically operates at 30% conversion efficiency with a gain bandwidth of  $1.5$  to  $2 \text{ cm}^{-1}$ . Peak powers of  $300 \text{ W}$  at average powers of  $30 \text{ mW}$  are typical operating parameters. Although historically parametric oscillators have operated with small excess gain, the gain of  $\text{LiNbO}_3$  parametric oscillators may be so high that they may find application as single pass parametric amplifiers. For example, recently a single pass gain of  $60 \text{ db}$  was measured experimentally for a  $.695 \mu$  pumped  $\text{LiNbO}_3$  crystal  $5 \text{ cm}$  long. The amplifier was used to amplify a  $1 \text{ mW}$   $1.15 \mu$  HeNe laser source to  $1 \text{ kW}$  peak power. The  $1 \text{ kW}$  output pulse represented 10% of the input pump power. As expected the amplifier showed temporal pulse narrowing of the amplified  $1.15 \mu$  HeNe source to one third of the  $60 \text{ nsec}$  pump pulse length. Simultaneous spatial narrowing was also observed. The potential applications for such a high gain amplifier include amplification of

low power narrow bandwidth diode laser sources for saturation spectroscopy, and amplification of infrared sources prior to detection by dark current limited infrared detectors. Investigations along these lines are continuing.<sup>12</sup>

Although  $\text{LiNbO}_3$  is transparent to  $5 \mu$  parametric oscillation becomes increasingly more difficult beyond  $3.5 \mu$  due to decreasing gain. Recently infrared parametric oscillation has been demonstrated in  $\text{CdSe}$ <sup>6</sup> and proustite.<sup>7,13,19</sup> However, neither of these materials are available with adequate crystal length for convenient oscillator operation. An additional limitation to infrared oscillator operation is the lack of a "fused-silica" type mirror substrate material and high optical quality dielectric coatings. These difficulties have combined such that infrared generation by mixing appears to be the more favorable route to a widely tunable infrared source.

The output power obtained by mixing is

$$\left( \frac{P_1}{P_2} \right) = \frac{\omega_1}{\omega_2} \Gamma^2 \ell^2 \text{sinc}^2 \left( \frac{\Delta k \ell}{2} \right) \quad (24)$$

Thus, though visible dye lasers may be convenient tunable sources there are not the optimum pump source for mixing for two reasons: the reduction in mixing efficiency by the Manley-Rowe factor, and the transparency requirements in both the infrared and visible for the nonlinear material. For infrared generation by mixing, the  $\text{LiNbO}_3$  parametric oscillator more closely fits the source requirements.

We have recently performed two mixing experiments to illustrate the advantages of widely tunable infrared generation by mixing. Figure 2 shows the wavelengths obtained by mixing in  $\text{CdSe}$ . The tunable pump source was two

$\text{LiNbO}_3$  oscillators operating within the same optical cavity pumped by  $.695 \mu$ . One crystal was tuned while the other was held fixed at  $1.833 \mu$ . The mixer phasematched between  $9.6 \mu$  and  $25 \mu$ . However, the detector response cut-off at  $13.5 \mu$ .

$\text{CdSe}$  is unique in that it has a wide transparency range  $.75 \mu - 25 \mu$  and  $70 \mu$  to submillimeter wavelengths combined with a large nonlinear coefficient and high crystal quality. The small birefringence of  $\text{CdSe}$  allows phasematched far infrared generation as shown in Fig. 3. However, the birefringence is inadequate for phasematching across the entire near infrared. For this spectral region crystals belonging to the chalcopyrite group appear particularly useful.

The nonlinear and phasematching properties of the ternary II - IV -  $\text{V}_2$  and I - III -  $\text{IV}_2$  chalcopyrite ( $\bar{4}2\text{m}$  point group) crystals have been determined. At this time four of the thirty compounds appear particularly useful for infrared nonlinear optical applications. These crystals are  $\text{AgGaS}_2$ <sup>15</sup>,  $\text{AgGaSe}_2$ <sup>16</sup>,  $\text{ZnGeP}_2$ <sup>17</sup> and  $\text{CdGeAs}_2$ <sup>18</sup>. The properties of these crystals including phasematching are reviewed in reference 3. Table I lists their nonlinear properties and transparency ranges. In general, the chalcopyrites have a very high nonlinearity.  $\text{AgGaS}_2$  and  $\text{ZnGeP}_2$  are transparent between  $.6 - 12 \mu$  and  $.7 - 12 \mu$  respectively.

We have concentrated our efforts on  $\text{AgGaSe}_2$  and  $\text{CdGeAs}_2$ <sup>19</sup> due to their extended infrared transparency  $.7 - 18 \mu$  and  $2.3 - 18 \mu$  and unique phase-matching properties. In addition,  $\text{AgGaSe}_2$  shows useful crystal growth properties and is available in reasonable quality crystals over  $1 \text{ cm}^3$  in volume.<sup>20</sup>

Figure 4 shows the  $7\ \mu$  to  $15\ \mu$  tuning range generated by mixing in  $\text{AgGaSe}_2$ . The output bandwidth was less than  $2\ \text{cm}^{-1}$  reflecting the bandwidth of the  $.695\ \mu$  pumped  $\text{LiNbO}_3$  parametric oscillator source. The unique features of this experiment were its simplicity and rapid, continuous tuning. The experimental arrangement consisted of collinear geometry with a Q-switch Nd:YAG laser operating at  $1.32\ \mu$  internally doubled with  $\text{LiIO}_3$  to generate  $.659\ \mu$ . The  $.659\ \mu$  pumped the singly resonant  $\text{LiNbO}_3$  parametric oscillator. The oscillator output mixed in the  $\text{AgGaSe}_2$  with the collinear  $1.32\ \mu$  with phasematching achieved by proper rotation of the  $\text{AgGaSe}_2$  crystal. Figure 5 shows a

phasematching angle. The  $\text{LiNbO}_3$  temperature scanned at  $1^\circ\text{C}/\text{min}$  and the  $\text{AgGaSe}_2$  synchronously rotated to continuously tune  $7.5\ \mu$  to  $12\ \mu$  in 10 minutes. The scanning was repeatable with approximately a 10% peak to peak fluctuation in output pulses and a signal to noise greater than 1000 in the HgCdTe detector. A demonstration polystyrene spectrum was scanned to illustrate the repeatability of this coherent spectrometer.

The above description of tuning ranges illustrates that it is now possible with only three nonlinear crystals and a Q-switched Nd:YAG laser source to generate  $.6\ \mu$  to  $3.5\ \mu$  by parametric oscillation in  $\text{LiNbO}_3$ ,  $3\ \mu$  to  $18\ \mu$  by mixing in  $\text{AgGaSe}_2$  and  $10\ \mu$  to  $25\ \mu$  and  $70\ \mu$  to  $1000\ \mu$  by mixing in  $\text{CdSe}$ . The question of bandwidth and frequency control is the next important question in spectroscopic application of these sources.

### III. BANDWIDTH

The gain bandwidth of a parametric oscillator is determined by the  $\text{sinc}^2\left(\frac{\Delta k l}{2}\right)$  phasematching factor. Expanding  $\Delta k$  in terms of frequency



and letting

$$\frac{\Delta k \ell}{2} = \pi \quad (25)$$

define the bandwidth we have

$$\Delta \nu (\text{cm}^{-1}) = \frac{1}{c \beta_{12} \ell} \quad (26)$$

where

$$\begin{aligned} \beta_{12} &= \left| \frac{\partial k_1}{\partial \omega_1} - \frac{\partial k_2}{\partial \omega_2} \right| \\ &= \frac{1}{c} \left[ n_2 - n_1 + \lambda_1 \frac{\partial n_1}{\partial \lambda_1} - \lambda_2 \frac{\partial n_2}{\partial \lambda_2} \right] \\ &\approx \frac{\Delta n}{c} \end{aligned} \quad (27)$$

Thus the gain bandwidth is approximately given by

$$\Delta \nu (\text{cm}^{-1}) \sim \frac{1}{\Delta n \ell} \quad (28)$$

where  $\Delta n$  is the crystal birefringence. Figure 6 shows the measured gain bandwidth of a  $.659 \mu$  pumped  $\text{LiNbO}_3$  singly resonant oscillator.

Similar to other coherent sources, the parametric oscillator can be frequency narrowed to oscillate in a single axial mode. The frequency narrowing methods include thermally tuned etalon,<sup>21</sup> tilted etalon,<sup>22</sup> Smith and the dual Smith interferometer<sup>23</sup> and birefringent filter.<sup>24</sup> The first

three methods have been demonstrated with good results. For example, Wallace<sup>21</sup> reports that a  $.92 \text{ cm}^{-1}$  free spectral range, finesse of 7.8, thermally tuned etalon effectively controls the oscillator bandwidth to a single axial mode with long term frequency stability of 30 MHz or  $0.001 \text{ cm}^{-1}$ . The commercial  $\text{LiNbO}_3$  parametric oscillator is available with this frequency control option and has been used in a series of experiments.<sup>26</sup> The use of a thermally tuned etalon is dictated by the small parametric oscillator cavity spot size which does not permit tilted etalon use.<sup>27</sup> The disadvantage of the thermal etalon is the slow thermal time constant and difficulty in stabilizing the etalon at the frequency of interest.

These thermally tuned etalon difficulties can be overcome by using a beam expanding telescope within the oscillator cavity to permit the use of a tilted etalon. Recently experiments were performed to demonstrate this frequency narrowing method.<sup>22</sup> Figure 7 shows a schematic of refractive and reflective beam expanding telescopes. These telescopes used inexpensive Edmonds optics but operated satisfactorily to expand the beam from  $100 \mu$  to  $600 \mu$ . Figure 8 shows the tuning capability achieved with a  $2.85 \text{ cm}^{-1}$  free spectral range, finesse of four tilted etalon. The bandwidth was less than the  $0.5 \text{ cm}^{-1}$  spectrometer resolution. Based on previous work with thermal etalons, bandwidth narrowing should be less than  $0.1 \text{ cm}^{-1}$  and approaching single frequency operation. The  $2.85 \text{ cm}^{-1}$  interval could be rapidly scanned in a convenient and repeatable manner illustrating the advantage of the tilted etalon. The use of a beam expanding telescope is required for the present confocally focused low power  $\text{LiNbO}_3$  oscillators. Operation of higher power oscillators dictates a larger oscillator cavity mode radius so that the beam expander would not be necessary.

Although birefringent elements have been proposed for use in parametric oscillators,<sup>24</sup> they have not yet been demonstrated. However experiments are presently in progress and based on their hoped for positive results, a combination birefringent filter and tilted etalon may provide the most convenient frequency narrowing method for future parametric oscillator devices.

#### IV. APPLICATIONS TO SPECTROSCOPY

Spectroscopic applications of tunable coherent sources covers a wide range of chemical, biological and physical systems. Rather than review the range of applications to which parametric oscillators have been applied, I will briefly describe our work which is related to remote air pollution monitoring using tunable infrared sources.<sup>28,29</sup>

Using a  $.532 \mu$  pumped  $\text{LiNbO}_3$  parametric oscillator operating in the  $2.3 \mu$  region, we have measured pressure broadening and absorption coefficients of the  $V'' = 0 \rightarrow V' = 2$  CO overtone transition.<sup>30</sup> Figure 9 illustrates the observed absorption spectrum taken by continuously scanning the oscillator wavelength with a resolution of  $0.1 \text{ cm}^{-1}$ . The detection system used is a dual differential boxcar integrator followed by ratio electronics.

Figure 10 shows the measured absorption coefficient and cross section vs CO pressure for the overtone transition. Similar data was taken for nitrogen pressure broadened CO up to 1 atm pressure. Extending the results to higher pressures is illustrated by Fig. 11.

Using the observed absorption spectra, the pressure broadening in CO is determined to be  $0.62 \times 10^{-3} \text{ cm}^{-1} \text{ Torr}^{-1}$  for the  $V'' = 0 \rightarrow V' = 2$  transition for the  $P(2) - P(4)$  rotational levels.

The above discussion illustrates just one application of parametric sources. As the tuning range, output energy and bandwidth improve a wider use of parametric devices can be expected. In particular, applications to long path spectroscopy,<sup>31</sup> chemical transfer rate spectroscopy<sup>26</sup> and optical pumping spectroscopy<sup>32</sup> can be expected.

## V. FUTURE DEVELOPMENTS

If I may speculate for a moment, I would like to describe a potential coherent infrared source that looks particularly promising. The system is based on a Nd:AG oscillator-amplifier pump source operating Q-switched at  $1.06 \mu$ . This source is capable of 400 mJ output at up to 40 pps.<sup>33</sup> Figure 12 shows the computed tuning curve for a  $\text{LiNbO}_3$  parametric oscillator directly pumped by  $1.06 \mu$ .<sup>34,35</sup> The output of this oscillator provides an ideal match to the phasematching properties of  $\text{AgGaSe}_2$ . Figure 13 illustrates the resulting tuning range achieved by mixing. Of particular interest from the device standpoint, is rapid tuning by crystal rotation and the requirement for only one set of mirrors reflecting between  $1.6 \mu$  and  $2.1 \mu$  for the  $\text{LiNbO}_3$  singly resonant oscillator. These phasematching curves illustrate the potential for a high energy continuously tunable  $1.6 \mu$  to  $18 \mu$  source based on well developed Nd:YAG laser and  $\text{LiNbO}_3$  oscillator technology.

In conclusion, parametric oscillator and mixing sources are now finding their way out of the laboratory and into an increasing number of spectroscopic applications. Their convenient operating characteristics, relatively high peak power and adequate bandwidth control coupled with a very wide tuning range assure increased future application as tunable coherent sources.

## REFERENCES

1. S.E. Harris, "Tunable Optical Parametric Oscillators", Proc. IEEE, 57, 2096, (1969).
2. R.G. Smith, "Optical Parametric Oscillators", Vol. 4 of Advances in Lasers, ed by A.K. Levine and A.J. De Maria, (to be published).
3. R.L. Byer, "Optical Parametric Oscillators", Treatise in Quantum Electronics, eds. H. Rabin and C.L. Tang, (1973), (to be published).
4. J.M. Yarborough and G.A. Massey, "Efficient High Gain Parametric Generation in ADP Continuously Tunable Across the Visible Spectrum", Appl. Phys. Lett. 18, 438, (1971).
5. R.W. Wallace, "Stable, Efficient Optical Parametric Oscillators Pumped with Doubled Nd:YAG", Appl. Phys. Lett. 17, 497, (1970).
6. R.L. Herbst and R.L. Byer, "CdSe Infrared Parametric Oscillator", Appl. Phys. Lett. 21, 189, (1972).
7. D.C. Hanna, B. Luther-Davies, R.C. Smith, "Singly Resonant Proustite Parametric Oscillator Tuned from 1.22  $\mu\text{m}$  to 8.5  $\mu\text{m}$ ", Appl. Phys. Lett. vol. 22, 440, (1973).
8. R.W. Wallace and S.E. Harris, "Extending the Tunability Spectrum", Laser Focus, Nov. 1970, p.42; also Chromatix Inc., Mountain View, Cal.



9. G.D. Boyd and D.A. Kleinman, "Parametric Interaction of Focused Gaussian Light Beams", J. Appl. Phys. 39, 3597, (1968).
10. G.D. Boyd and A. Ashkin, "Theory of Parametric Oscillator Threshold with Single-Mode Optical Masers and Observation of Amplification in  $\text{LiNbO}_3$ ", Phys. Rev. 146, 187, (1966).
11. J.F. Ready, Effects of High Power Laser Radiation, Academic Press, New York, 1971.
12. R.L. Byer and R.L. Herbst, "High Gain  $\text{LiNbO}_3$  Parametric Amplifiers", (to be published).
13. E.O. Ammann and J.M. Yarborough, "Optical Parametric Oscillation in Proustite", Appl. Phys. Lett. 17, 233, (1970).
14. D.C. Hanna, B. Luther-Davies, H.N. Rutt and R.C. Smith, "Reliable Operation of a Proustite Parametric Oscillator", Appl. Phys. Lett. 20, 34, (1972).
15. D.S. Chemla, P.J. Kupecek, D.S. Robertson and R.C. Smith, "Silver Thiogallate, a New Material with Potential for Infrared Devices", Optic. Comm. I, 29, (1971).
16. G.D. Boyd, H.M. Kaspar, J.H. McFee and F.G. Stortz, "Linear and Nonlinear Optical Properties of some Ternary Selenides", IEEE J. Quant. Elect. QE-8, 900, (1972).

17. G.D. Boyd, E. Beuhler and F.G. Stortz, "Linear and Nonlinear Optical Properties of  $\text{ZnGeP}_2$  and  $\text{CdSe}$ ", Appl. Phys. Lett. 18, 301, (1971).
18. R.L. Byer, H. Kildal and R.S. Feigelson, " $\text{CdGeAs}_2$  - A New Nonlinear Crystal Phasematchable at  $10.6 \mu\text{m}$ ", Appl. Phys. Lett. 19, 237, (1971).
19. H. Kildal, R.F. Begley, M.M. Choy and R.L. Byer, "Efficient Second and Third Harmonic Generation of  $10.6 \mu\text{m}$  in  $\text{CdGeAs}_2$ ", J. Opt. Soc. of Am. 62, 1398, (1972).
20. H. Kildal, (private communication).
21. R.W. Wallace, IEEE Conf. on Laser Application, Washington, D.C. (1971).
22. R.L. Herbst and R.L. Byer, "Line Narrowing of a  $\text{LiNbO}_3$  Parametric Oscillator Using a Tilted Etalon", (to be published).
23. J. Pinard and J.F. Young, "Interferometric Stabilization of an Optical Parametric Oscillator", Optic Comm. 4, 425, (1972).
24. S.E. Harris, (private communication).
25. S.R. Leone and C.B. Moore, "Optical Parametric Oscillator Pumped Vibrational Energy Transfer Studies of Hydrogen Chloride", J. Opt. Soc. of Am. 62, 1358, (1972).
26. M. Hercher, "Tunable Single Mode Operation of Gas Lasers Using Intracavity Etalons", Appl. Optics. 8, 1103, (1969).

27. H. Kildal and R.L. Byer, "Comparison of Laser Methods for the Remote Detection of Atmospheric Pollutants", Proc. IEEE, 59, 1644, (1971).
28. R.L. Byer and M. Garbuny, "Pollutant Detection by Absorption Using Mie Scattering and Topographical Targets as Retroreflectors", Applied Optics, (July 1973).
29. M. Garbuny, T. Henningsen and R.L. Byer, "Experimental Studies for Remote Gas Detection by Parametric Laser Tuning", Spring Meeting Optical Society of America, Denver, Colo. March, 1973.
30. V. Vali, R. Goldstein and K. Fox, "Very Long-Path Absorption Cell for Molecular Spectroscopy", Appl. Phys. Lett. 22, 391, (1973).
31. T.Y. Chang and O.R. Wood, "Optically Pumped N<sub>2</sub>O Laser, Appl. Phys. Lett. 22, 93, (1973).
32. M. Yarborough, (private communication).
33. E.O. Ammann, J.D. Foster, M.K. Oshman and J.M. Yarborough, "Repetively Pumped Parametric Oscillator at 2.13  $\mu$ m", Appl. Phys. Lett. 15, 131, (1969).
34. E.O. Ammann, J.M. Yarborough and J. Falk, "Simultaneous Optical Parametric Oscillation and Second Harmonic Generation", J. Appl. Phys. 42, 5618, (1971).

# FIGURE CAPTIONS

1. Experimental tuning curves for a  $0.659\text{ }\mu\text{m}$  pumped  $\text{LiNbO}_3$  parametric oscillator. Also shown are the up-converted wavelengths obtained with an internal  $\text{LiIO}_3$  crystal.
2. Measured difference output in  $\text{CdSe}$ . The tunable pump source was 2  $\text{LiNbO}_3$  SRO operating within a single cavity pumped by  $0.659\text{ }\mu\text{m}$  of a doubled  $\text{Nd:YAG}$  laser. One oscillator was tuned while the second was held at  $1.833\text{ }\mu\text{m}$ .
3. Far infrared phasematching in  $\text{CdSe}$ .
4.  $7\text{ }\mu - 15\text{ }\mu$  output in  $\text{AgGaSe}_2$  pumped by  $1.318\text{ }\mu$  mixed against a  $0.659\text{ }\mu$  pumped  $\text{LiNbO}_3$  parametric oscillator.
5. Plot of  $\text{AgGaSe}_2$  phasematching angle vs  $\text{LiNbO}_3$  parametric oscillator temperature showing the proper crystal rotation for  $7.5\text{ }\mu$  to  $12\text{ }\mu$  continuous tuning.
6. Measured bandwidth for a  $0.659\text{ }\mu\text{m}$  pumped  $\text{LiNbO}_3$  SRO. The calculated linewidth for the  $5\text{ cm}$  crystal is  $1.60\text{ cm}^{-1}$ .
7. Beam expanding telescopes to allow the use of a tilted etalon for frequency narrowing a  $\text{LiNbO}_3$  parametric oscillator.
8. Tilted etalon tuned  $0.659\text{ }\mu$  pumped  $\text{LiNbO}_3$  parametric oscillator. The etalon had a  $2.85\text{ cm}^{-1}$  free spectral range and a finesse of four.

9. CO overtone spectrum taken with a  $\text{LiNbO}_3$  parametric oscillator at  $.1 \text{ cm}^{-1}$  resolution at a 1 m absorption path length.
10. Absorption coefficient and cross sections at peak of P(3) line in  $V = 0 \rightarrow V = 2$  transition of CO.
11. Pressure broadening of the CO overtone transition.
12. Angle tuning curve for a  $1.06 \mu \text{ LiNbO}_3$  parametric oscillator.
13.  $3 - 18 \mu \text{ AgGaSe}_2$  mixing source pumped by a  $\text{LiNbO}_3$  singly resonant parametric oscillator.



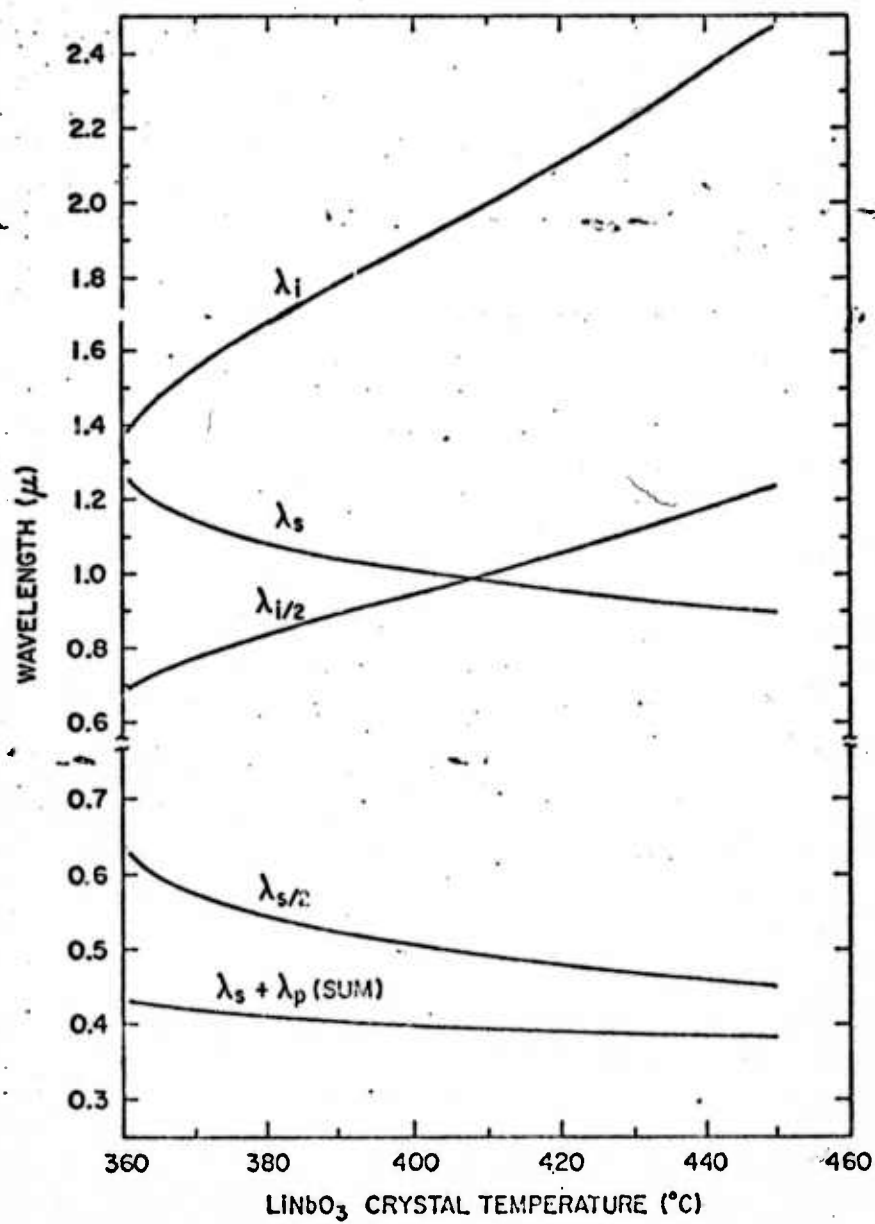


FIGURE 1

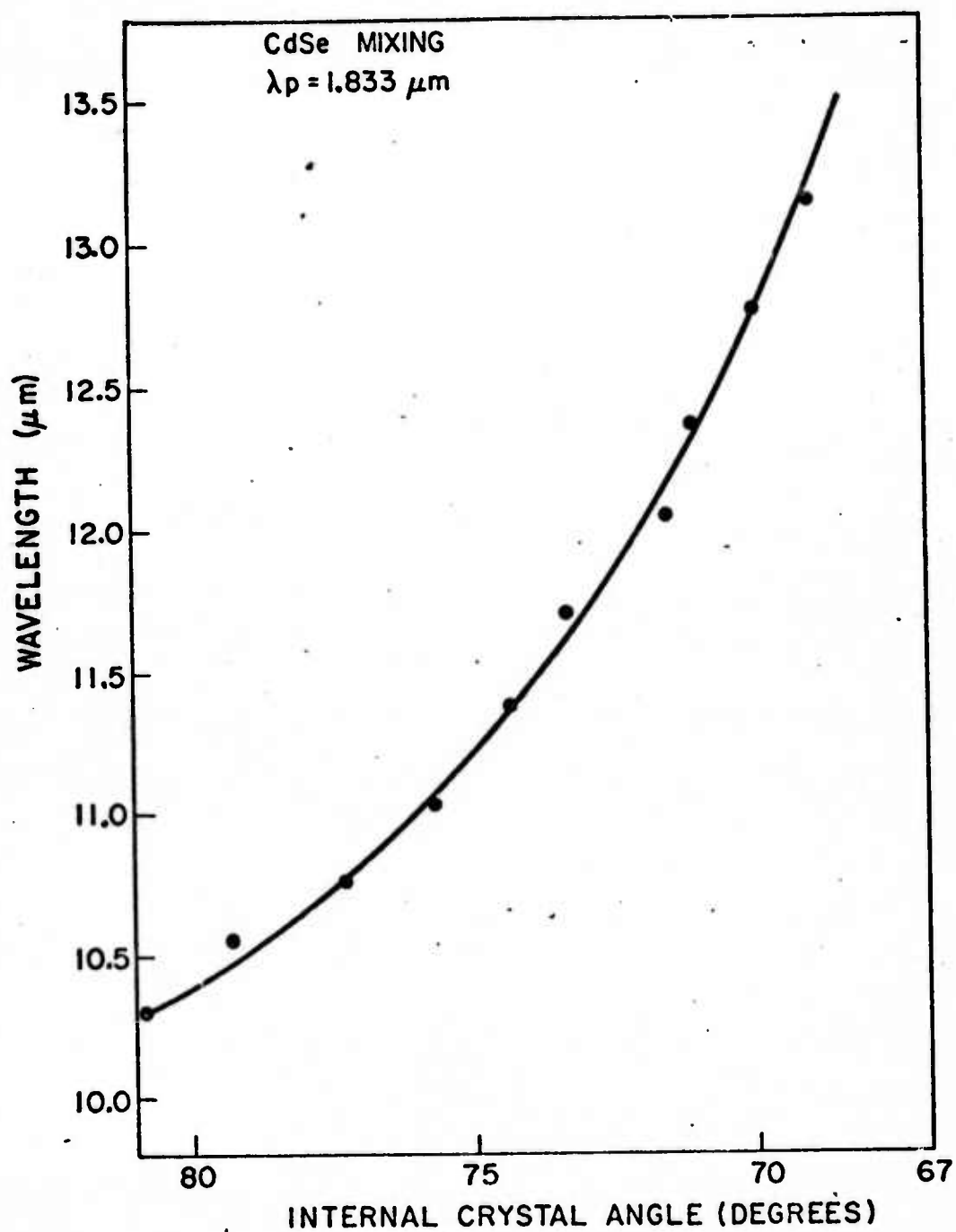
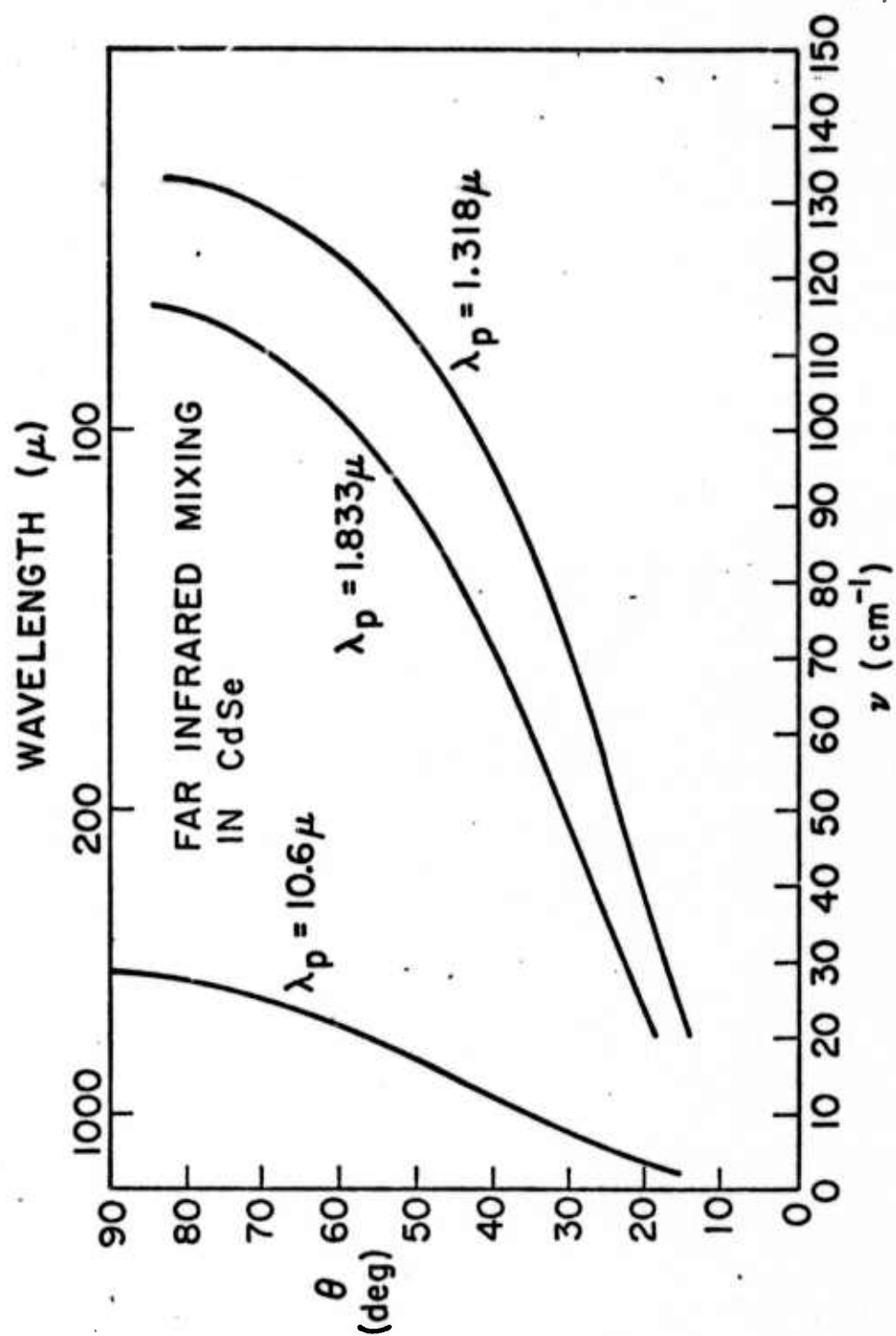


FIGURE 2



2808-3

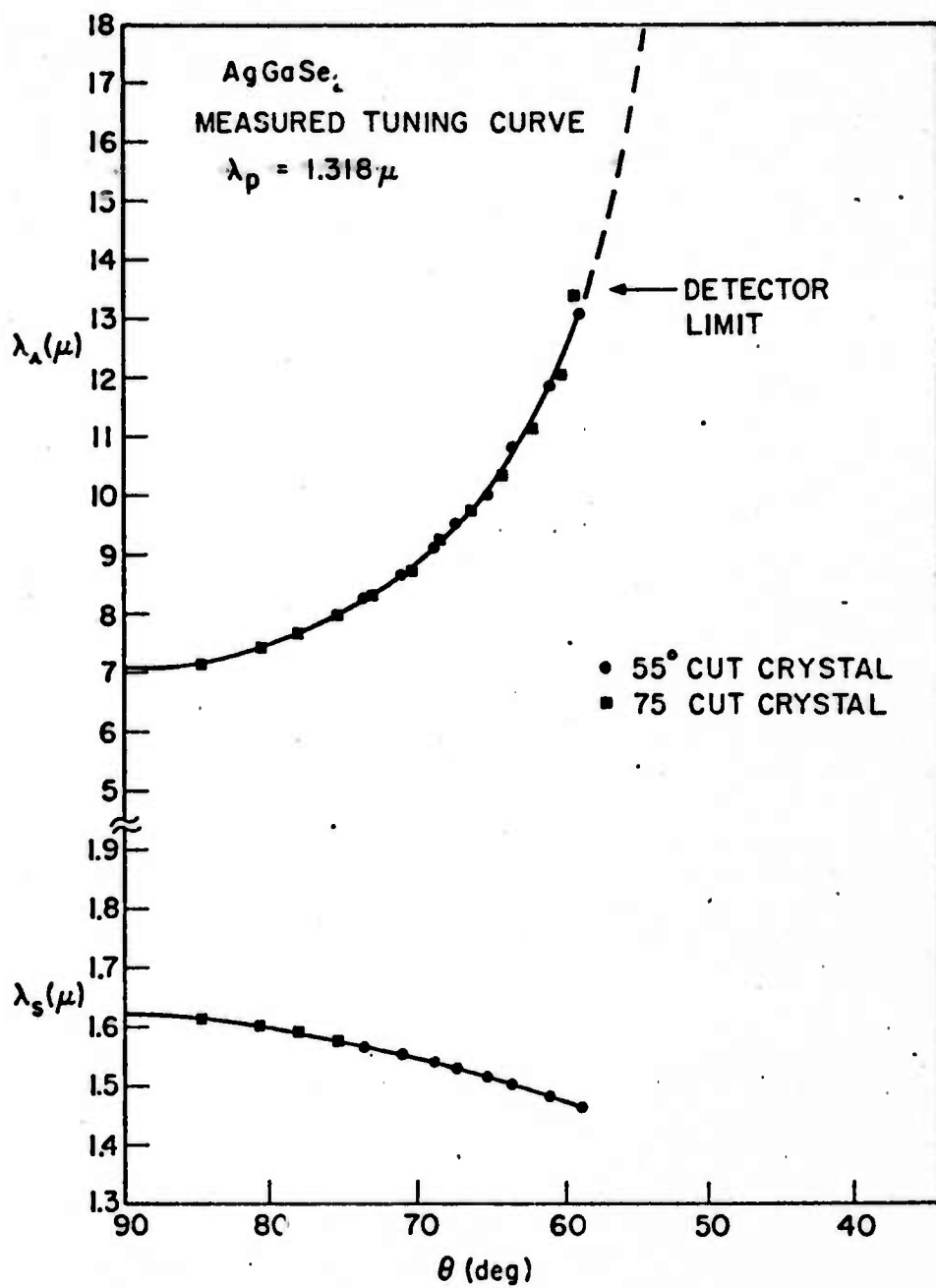


FIGURE 4

2508-4

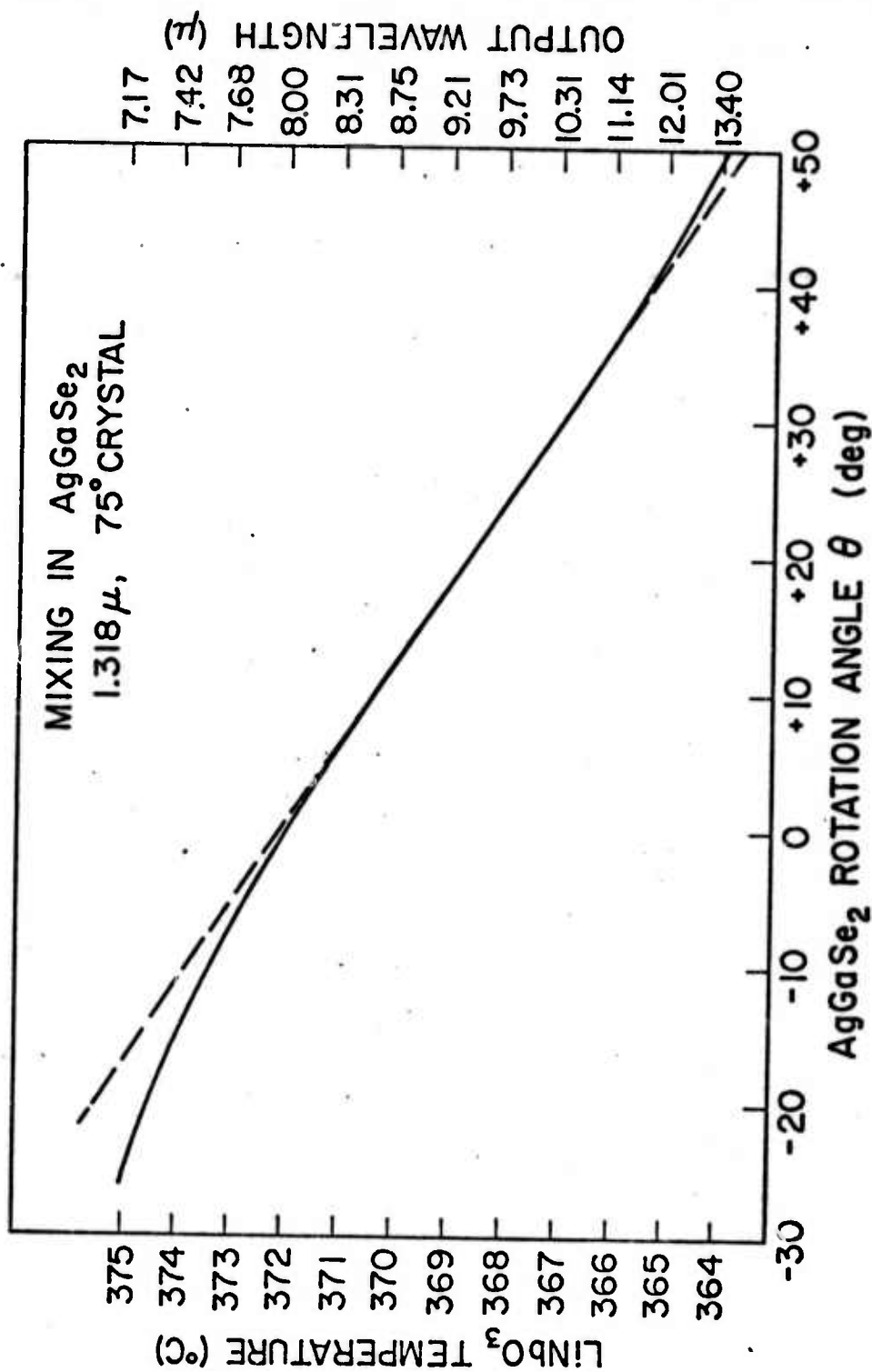


FIGURE 5



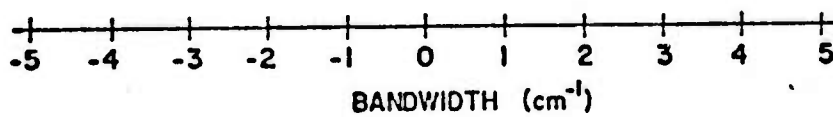
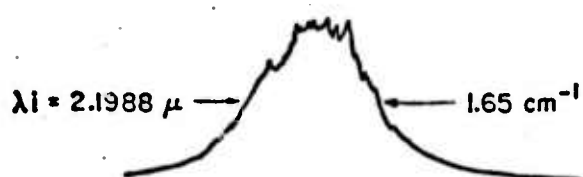
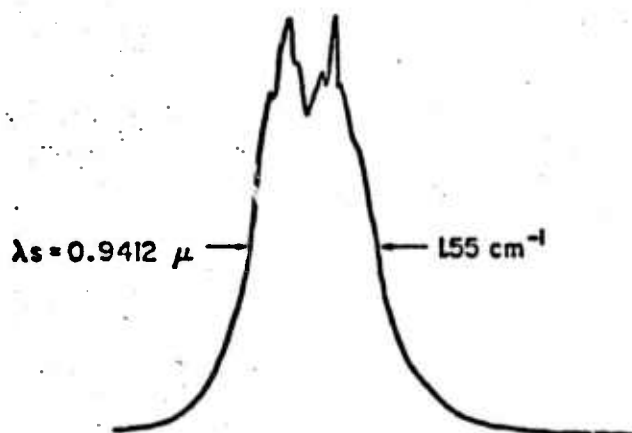
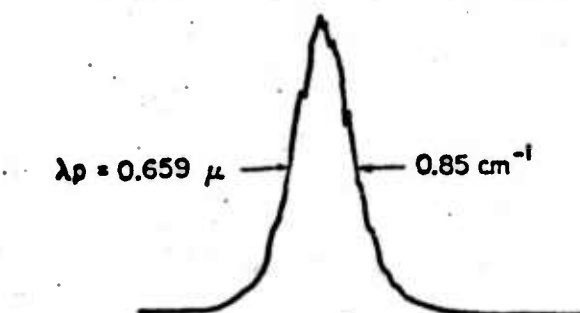
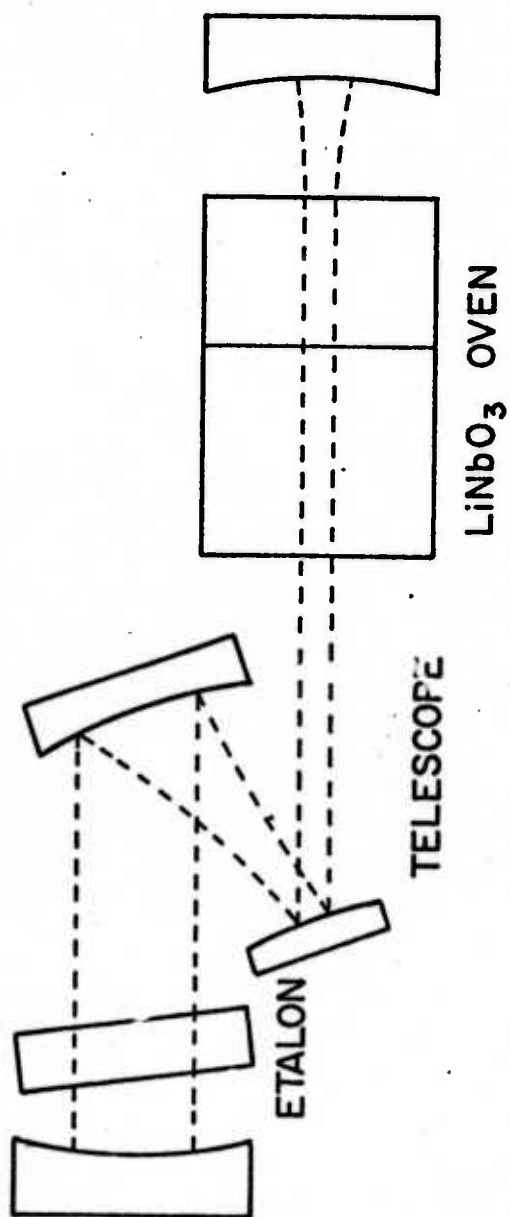
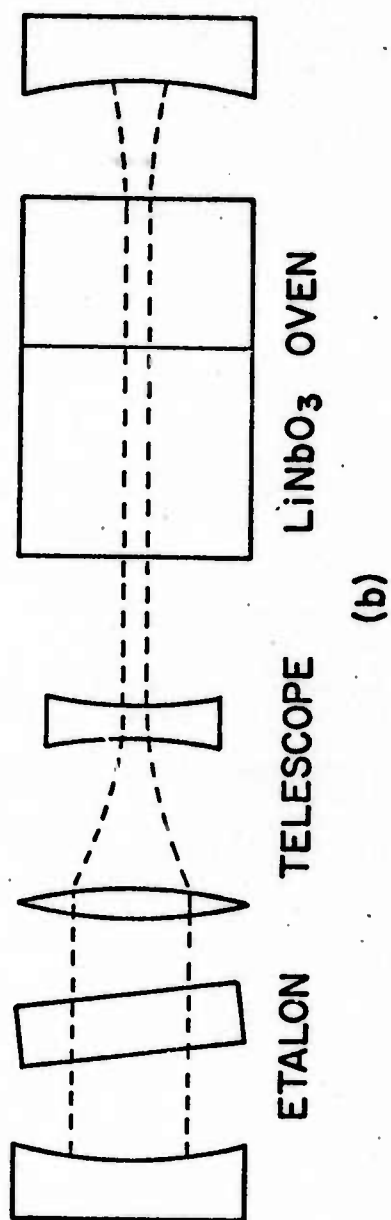


FIGURE 6

# ETALON NARROWED PARAMETRIC OSCILLATOR



(a)



(b)

FIGURE 7

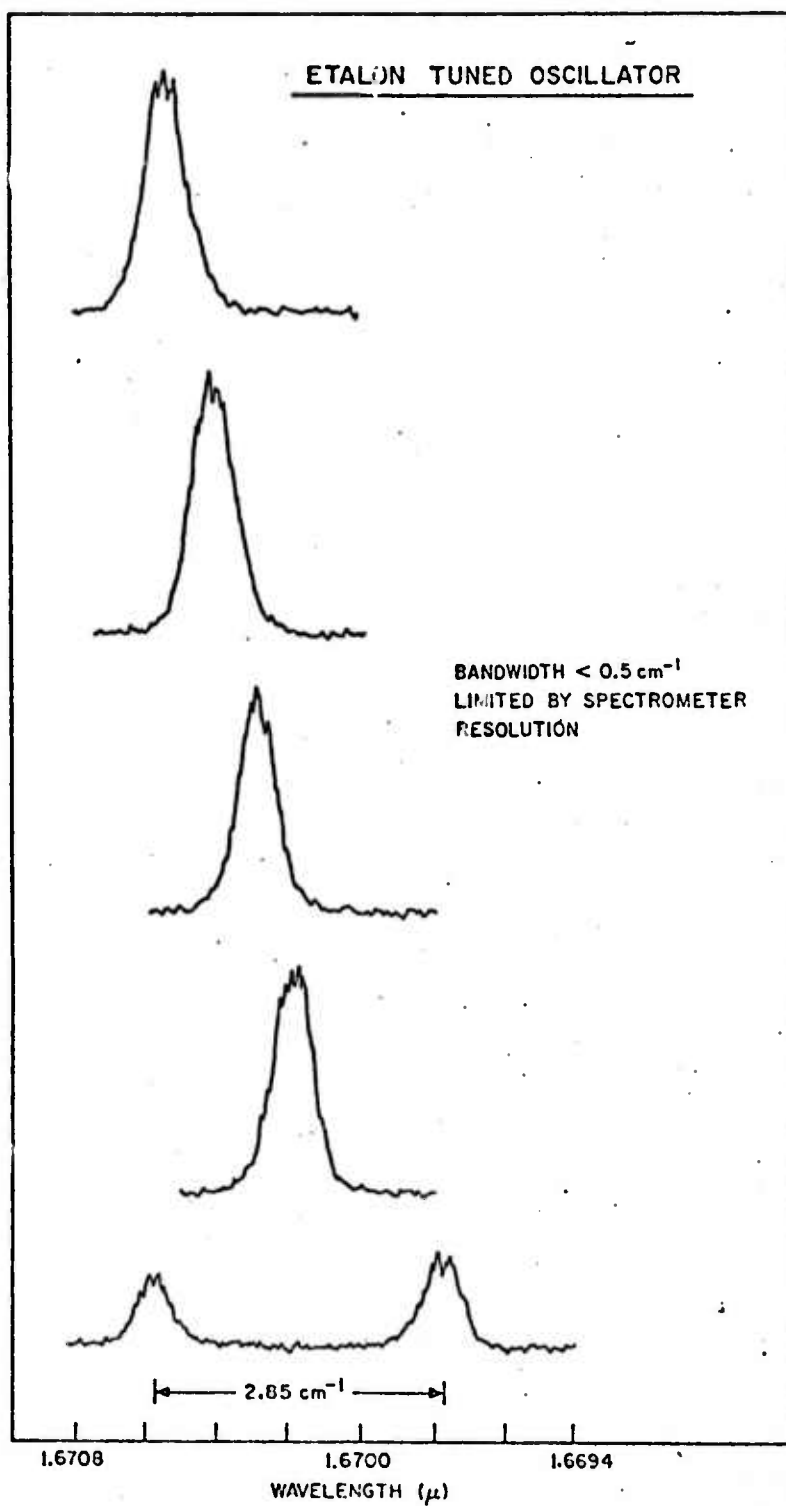


FIGURE 8

## CO OVERTONE SPECTRUM

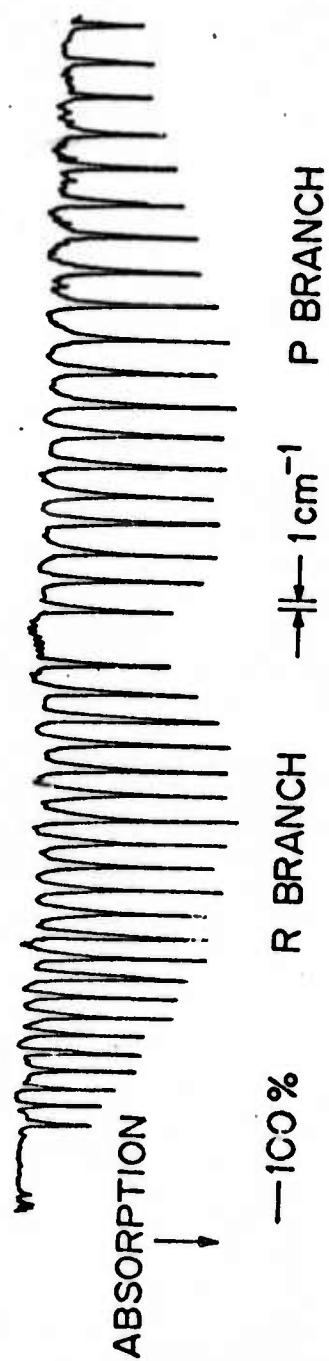
 $V'' = 0 \rightarrow V' = 2$  600 Torr

FIGURE 9.

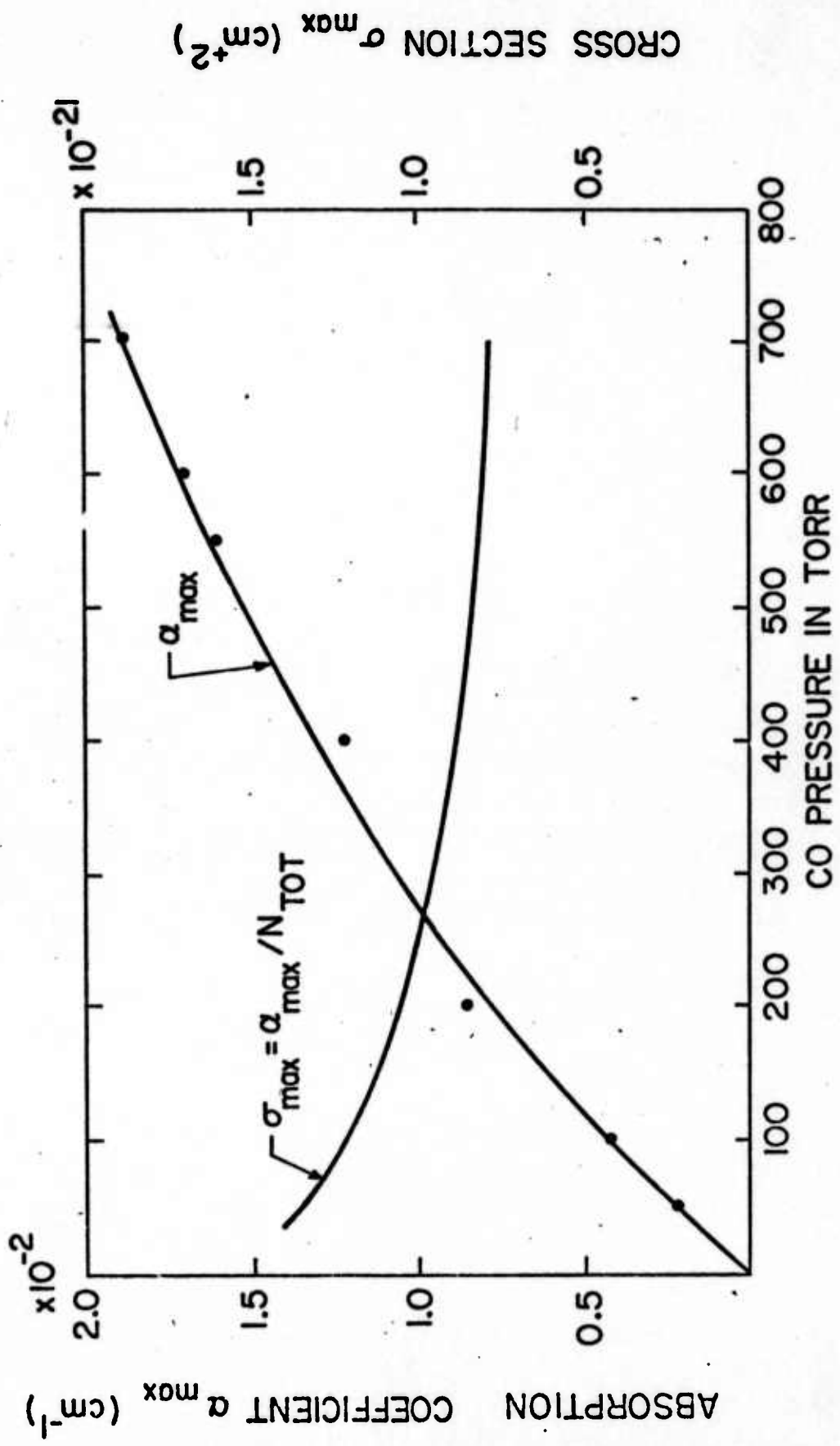


FIGURE 10

CO OVERTONE SPECTRUM

$$v''=0 \rightarrow v'=2$$

2802-5

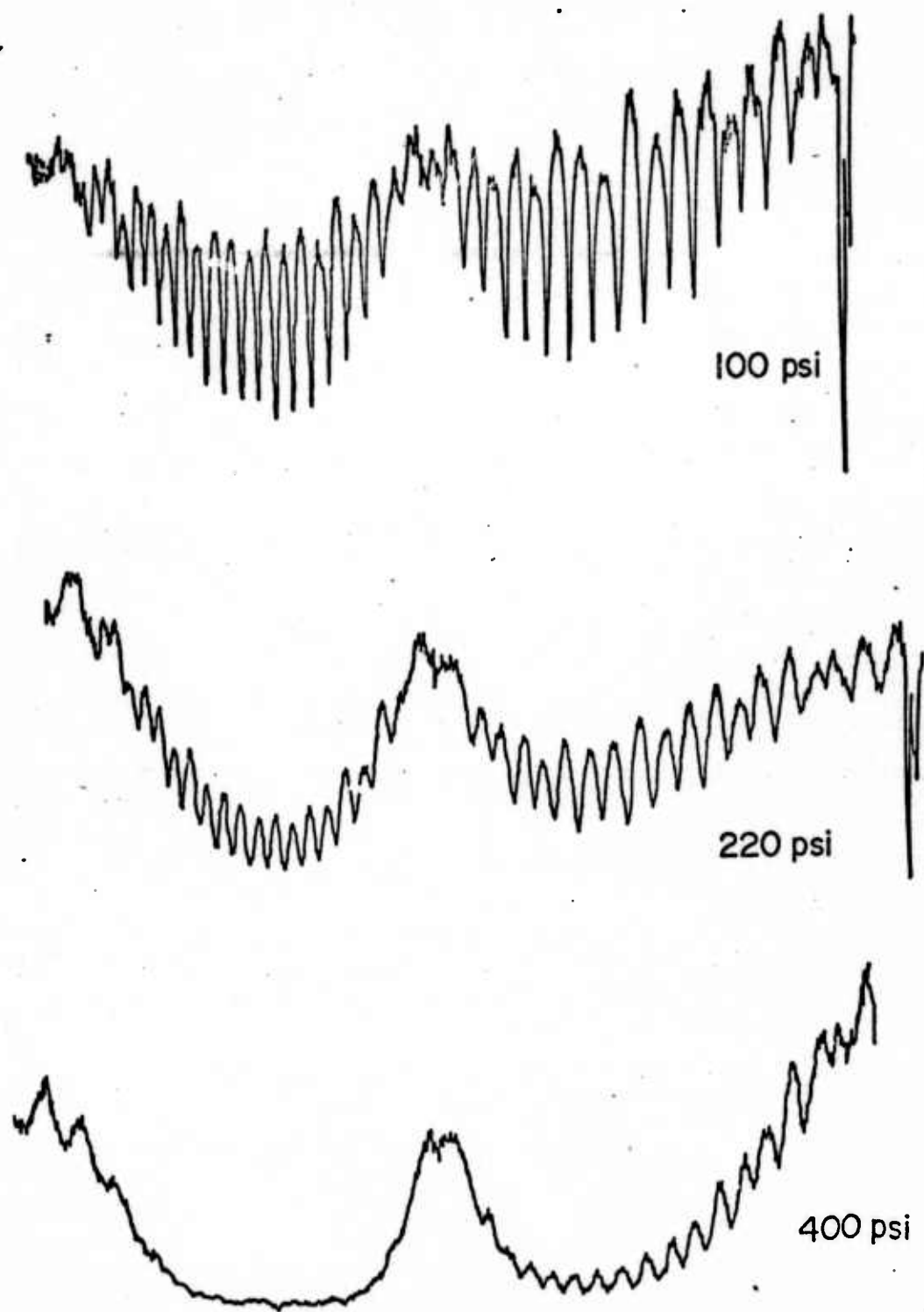


FIGURE 11



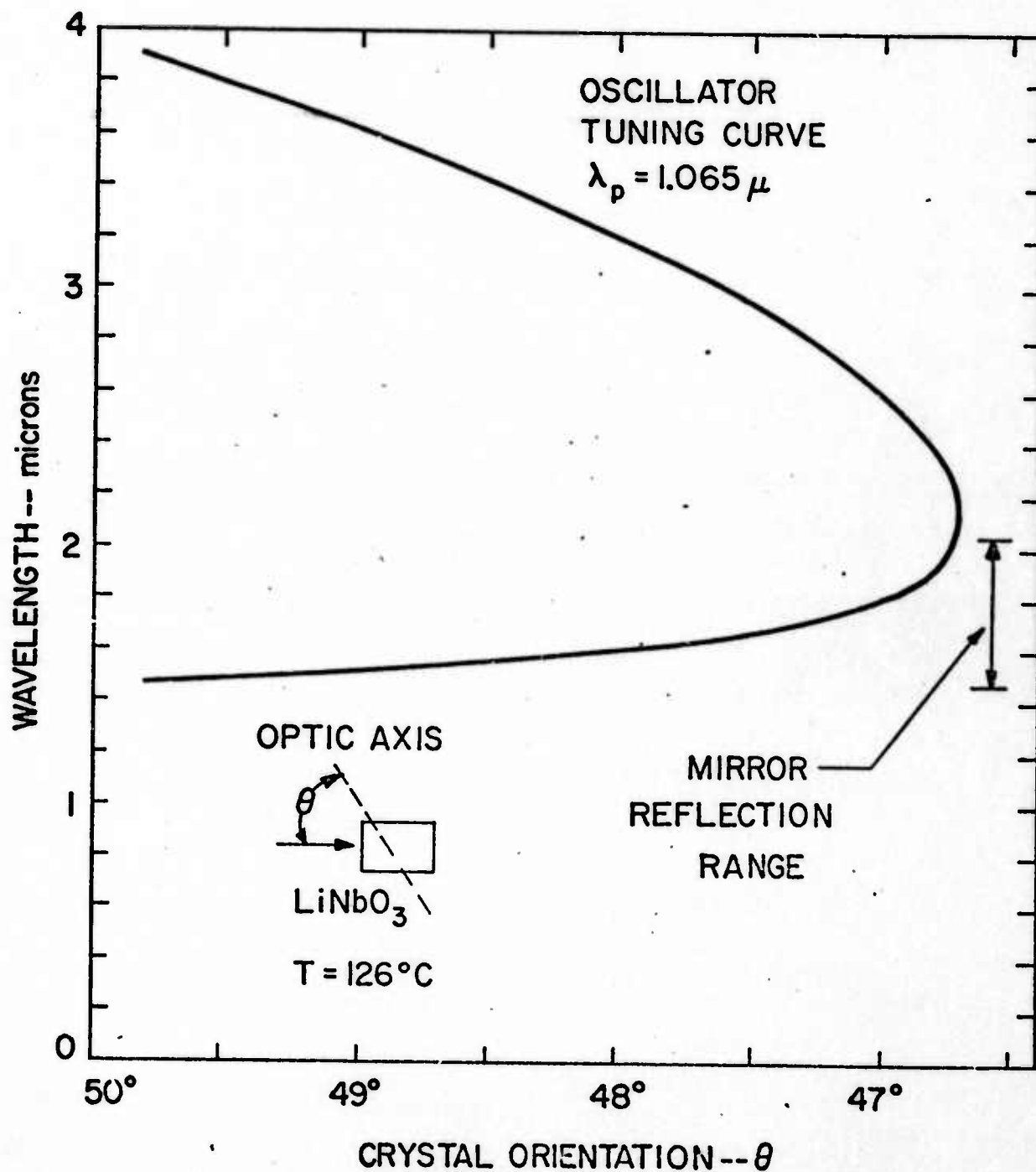


FIGURE 12

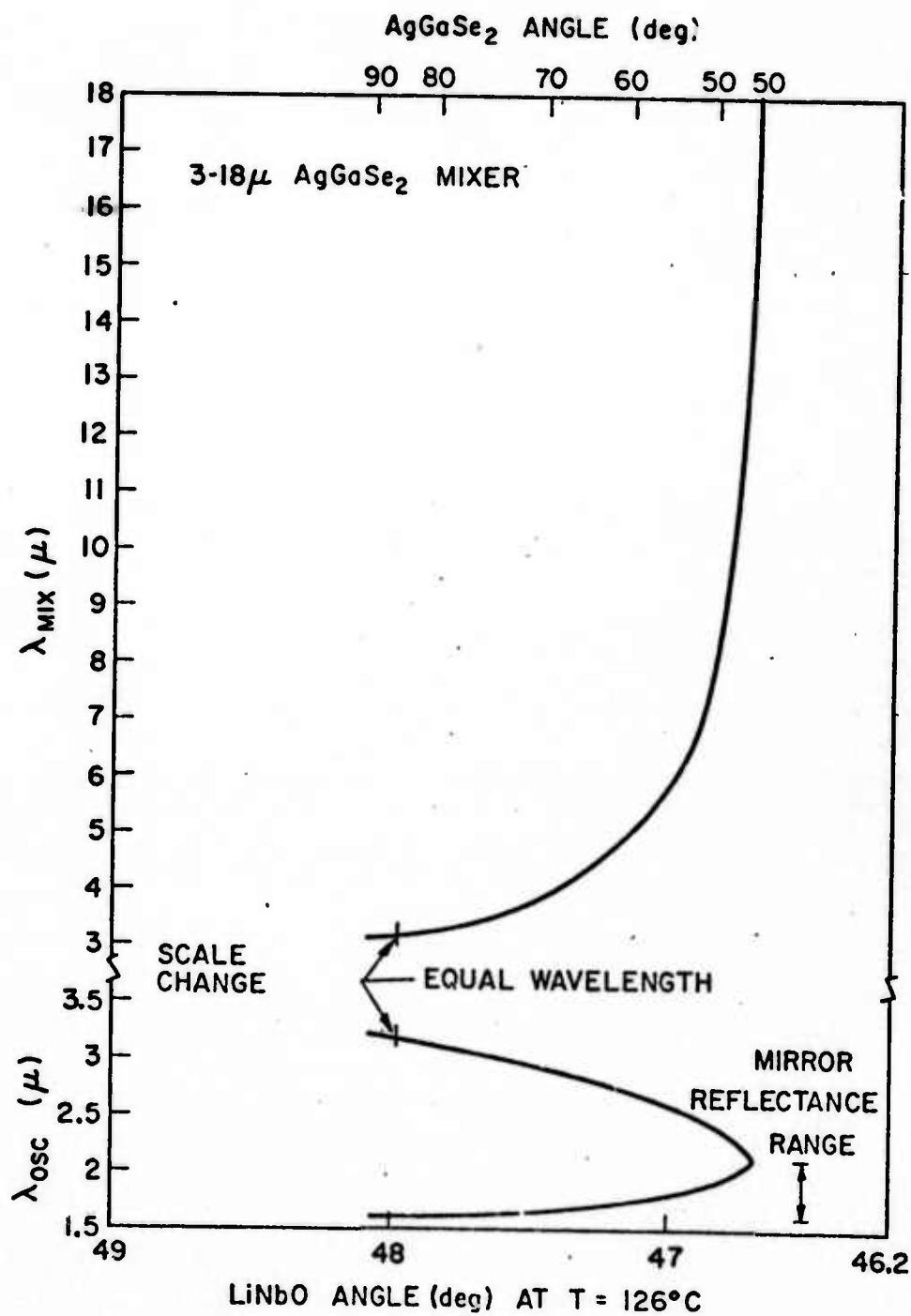


FIGURE 13

Reproduction in whole or in part is permitted by the publisher for any purpose of the United States Government.

# PHYSICAL REVIEW LETTERS

VOLUME 31

6 AUGUST 1973

NUMBER 6

## Generation of Vacuum-Ultraviolet and Soft-X-Ray Radiation Using High-Order Nonlinear Optical Polarizabilities\*

S. F. Harris

*Microwave Laboratory, Stanford University, Stanford, California 94305*

(Received 30 May 1973)

The harmonic or sum-frequency power generated in the last coherence length of a low-density atomic species is calculated subject to the condition that the applied electric field be bounded by the multiphoton absorption or ionization limit. It is shown that higher-order polarizations may equal or exceed lower-order polarizations. Calculations are given for generation at 1773 and 1064 Å in Xe, and at 236, 169, and 177 Å in Li<sup>+</sup>.

In recent years, picosecond-time-scale laser systems have evolved to the point where it is readily possible to produce focused optical pulses with power densities which are greater than the multiphoton ionization threshold of single atoms, and which at the same time have energy densities low enough that inverse bremsstrahlung (avalanche) ionization of the species does not occur.<sup>1</sup> By using the third-order nonlinear polarizability of low-pressure xenon, and operating at peak power densities which approach the multiphoton ionization limit ( $P/A \approx 5 \times 10^{12}$  W/cm<sup>2</sup>), picosecond laser pulses at 3547 Å have recently been used to produce third-harmonic radiation at a conversion efficiency of 3%.<sup>2</sup>

In this Letter, I consider the relative magnitude of the higher-order nonlinear optical polarizabilities; i.e.,  $\mathcal{P}^{(3)} \sim E^3$ ,  $\mathcal{P}^{(5)} \sim E^5$ ,  $\mathcal{P}^{(7)} \sim E^7$ , etc.; where the applied electric field strength,  $E$ , is bounded by the condition that it not exceed the multiphoton absorption or ionization limit of the atom. It is shown, for many practical systems where the electronic transition frequencies

to ground are greater than the frequency of the applied laser fields, that at incident power densities which approach the multiphoton ionization limit, the higher-order polarizations may equal or exceed lower-order polarizations. There is also often a basic invariance, where the harmonic or sum-frequency power generated in the last coherence length of an atomic species is independent of the position and oscillator strengths of the intermediate levels, and of the order of the nonlinear polarizability involved. As a first experimental test of these ideas, Kung *et al.* have recently demonstrated the fifth-harmonic process 5320 Å - 1064 Å in low-pressure xenon.<sup>3</sup>

We consider an atomic system with certain transition frequencies to ground denoted by  $\omega_{01}$ ,  $\omega_{02}$ , ...,  $\omega_{0n}$ . We assume that optical radiation at frequencies  $\omega_1$ ,  $\omega_2$ , ...,  $\omega_n$  is applied to the system (for  $n$ th-harmonic generation  $\omega_1 = \omega_2 = \dots = \omega_n$ ). We assume that a single path through the atomic levels dominates the nonlinear optical susceptibility. For a gas with  $N$  atoms/cm<sup>3</sup>, the dipole moment at the sum frequency  $\omega_s = \omega_1 + \omega_2 + \dots + \omega_n$  is approximately given by<sup>4</sup>

$$\mathcal{P}^n(\omega_s) = N \frac{\mu_{01}\mu_{12}\dots\mu_{(n-1)n}\mu_{n0}E(\omega_1)E(\omega_2)\dots E(\omega_n)}{\hbar^n(\omega_s - \omega_{01})(\omega_1 + \omega_2 - \omega_{02})\dots(\omega_s - \omega_{0n})}, \quad (1)$$

where  $\mu_{ij}$  are the dipole matrix elements connecting the various levels (0 denotes ground, and is the

only level which is populated). We calculate the power density  $P/A(\omega_s)$  which is generated in one coherence length at the sum frequency. (The coherence length is  $L_c = |\pi/\Delta k|$ , where  $\Delta k$  is the difference in the propagation vectors of the driving polarization and the free electromagnetic wave at  $\omega_s$ .) Experimentally, this is the power density which will be generated when a Gaussian laser beam is focused to the center of a negatively dispersive media with a confocal parameter equal to  $L_c$ .<sup>5,6</sup> We assume that the sum frequency  $\omega_s$  is sufficiently close to  $\omega_{0n}$  that this transition, by itself, approximately determines  $L_c$ ; then

$$L_c = 2\pi\hbar(\omega_s - \omega_{0n})/N\eta\omega_s\mu_{0n}^2, \quad (2)$$

where  $\eta = (\mu/\epsilon_0)^{1/2}$ . From Maxwell's equations, the power density generated in one coherence length of atoms is  $P/A(\omega_s) = (1/2\pi^2)\eta\omega_s^2[\delta(\omega_s)]^2L_c^2$ . Define  $\gamma_{ij} = (\mu_{ij}E_j/\hbar\Delta\omega_j)^2$ , where  $\Delta\omega_j = \omega_{0j} - \omega_1 - \omega_2 - \dots - \omega_j$ . Using Eqs. (1) and (2), the conversion efficiency from the highest applied frequency  $\omega_n$  to the sum frequency  $\omega_s$  is given by

$$\delta = \frac{P/A(\omega_s)}{P/A(\omega_n)} = 4\gamma_{01}\gamma_{12}\dots\gamma_{n-2,n-1}\frac{\mu_{n-1,n}^2}{\mu_{0n}^2}. \quad (3)$$

The maximum conversion efficiency to  $\omega_s$  is determined by the maximum allowed value of  $E(\omega_1), E(\omega_2), \dots, E(\omega_n)$ . These are assumed to be limited by the  $n$ th-order absorption probability  $W^{(n)}$  which, again subject to the assumption of a single dominant path, is given by<sup>7,8</sup>

$$W^{(n)} = \hbar^{-2}\gamma_{01}\gamma_{12}\dots\gamma_{n-2,n-1}\mu_{n-1,n}\rho_n E^2(\omega_n), \quad (4)$$

where  $\rho_n$  is the density of states of the upper transition. Note that the single-photon cross section for absorption of  $\omega_s$  by the transition  $\omega_{0n}$  is given by  $\sigma_{0n}(\omega_s) = \eta\omega_s\mu_{0n}^2\rho_n/2\hbar$ . Using Eq. (4), Eq. (3) may be written

$$\delta = \frac{\hbar\omega_s}{\sigma_{0n}(\omega_s)} \frac{W^{(n)}}{[P(\omega_n)/A]} = \frac{\hbar\omega_s}{2\sigma_{0n}(\omega_s)} \frac{1}{J(\omega_n)/A}, \quad (5)$$

where  $J(\omega_n)/A$  is the incident energy density at the highest applied frequency  $\omega_n$ . The second equality in Eq. (5) follows by multiplying numerator and denominator by the length of the laser pulse,  $\Delta t$ , and allowing the applied fields to increase until  $W^{(n)}\Delta t = \frac{1}{2}$ , i.e., 50% of the atoms are excited to the upper level. (It is assumed that  $\Delta t$  is shorter than the decay time of the upper level.) The quantity  $\hbar\omega_s/2\sigma_{0n}(\omega_s)$  is often termed the saturation energy density, and is that density which if incident from the outside would approximately saturate the transition.

Note that this conversion efficiency is independent of the order of the nonlinear polarizability, and also of the oscillator strengths and positions of the intermediate levels. If intermediate levels have smaller oscillator strengths or resonant denominators, the incident applied fields are allowed to increase to yield the same conversion efficiency.

The foregoing has assumed that the generated frequency  $\omega_s$  is sufficiently close to some upper level  $\omega_{0n}$ , and that this level both determines the coherence length and most severely limits the allowable incident power density. More generally, the maximum allowable power density will be determined by multiphoton absorption to some other discrete level, or, most often, by multiphoton ionization to the continuum. Equation (3) still applies, but the maximum allowable  $E$  fields are now shown to be determined by the condition that

$$\gamma_{01}\gamma_{12}\dots\gamma_{q-2,q-1} = \frac{1}{8} \frac{\hbar\omega_s}{\sigma_{q-1,q}} \frac{1}{J/A(\omega_s)}, \quad (6)$$

where  $q$  denotes that level or point in the continuum which most severely limits the allowable fields. The quantity  $\gamma_{01}\gamma_{12}\dots\gamma_{n-2,n-1}$  is then substituted into Eq. (3) to determine the conversion efficiency. [If  $q=n$ , then Eqs. (6) and (3) combine to give Eq. (5).]

Before applying the foregoing, two qualifications are in order. First, at the level of applied electric field strengths, Stark shifts may be significant. In principle, these can be included in the frequency denominators.<sup>9</sup> In practice, allowing that the electric field is a free variable, the predicted conversion efficiencies are not very sensitive to the exact position of the upper atomic levels. There are also certain questions with regard to the applicability of the perturbation theory at these high field strengths. These same questions apply to multiphoton ionization theories,<sup>7-9</sup> which experimentally have proven to be reasonably accurate.

As a first example, consider the third-harmonic process  $3547 \text{ \AA} - 1182 \text{ \AA}$  in xenon. To evaluate Eq. (6), I choose the four-photon path  $5p^6[1S]0-6s[1\frac{1}{2}]1-6p[0\frac{1}{2}]1-7s[1\frac{1}{2}]2$ -continuum<sup>8,10</sup> as that which will most severely bound the allowable incident power density. I assume unity oscillator strength for all transitions and estimate  $\sigma_{7s\text{-continuum}}$  at  $3 \times 10^{-10} \text{ cm}^2$ .<sup>8</sup> Then assuming an incident 30-psec pulse at  $3547 \text{ \AA}$  yields  $(P/A)_{\text{max}} = 1.32 \times 10^{12} \text{ W/cm}^2$ . At this density, Eq. (3) predicts a conversion efficiency of 0.34%. Experimentally, us-

TABLE I. Conversion efficiency and limiting power density for some higher-order nonlinear processes.

Process	Species and path	Limiting $P/A$ (W/cm <sup>2</sup> )	Conversion efficiency (%)
$3 \times 5320 \text{ \AA} \rightarrow 1773 \text{ \AA}$	Xe <sup>a</sup> , $5p-6s-5p-6s-6p-8d-c$	$1.94 \times 10^{12}$	0.084
$5 \times 5320 \text{ \AA} \rightarrow 1064 \text{ \AA}$	As above	As above	0.051
$5 \times 1182 \text{ \AA} \rightarrow 236 \text{ \AA}$	Li <sup>b</sup> , $1s-2p-1s-2p-3s-2p-3s-4p-c$	$1.68 \times 10^{15}$	0.002
$7 \times 1182 \text{ \AA} \rightarrow 169 \text{ \AA}$	As above	As above	0.004
$15 \times 2660 \text{ \AA} \rightarrow 177 \text{ \AA}$	Li <sup>c</sup> , $(1s-2p)^7-(2p-3s)^7-3p-4d-c$	$3.47 \times 10^{15}$	$4 \times 10^{-7}$

<sup>a</sup> $5p=5p[{}^1S]0$ ;  $6s=6s[{}^1S]1$ ;  $6p=6p[{}^2P]2$ ;  $8d=8d[{}^2D]3$ ;  $c$ =continuum.

<sup>b</sup> $1s=1s[{}^1S]0$ ;  $2p=2p[{}^1P]1$ ;  $3s=3s[{}^1S]0$ ;  $4p=4p[{}^1P]1$ ;  $c$ =continuum.

<sup>c</sup> $3p=3p[{}^1P]1$ , others as in b.

ing tight focusing to the center of a xenon cell at a pressure of 3 Torr, a conversion efficiency of 0.9% has been measured.<sup>2</sup>

A number of other examples of the theory are summarized in Table I. The first two are concerned with generation of vacuum ultraviolet radiation in Xe. Assuming an incident laser pulse with a peak power of  $10^6$  W, then to exceed the multiphoton ionization limit we must focus to an area less than about  $5 \times 10^{-5}$  cm<sup>2</sup>, and thus (at 5320 Å) to a confocal parameter less than 3.7 cm. For focusing to the center of a negatively dispersive media we set the coherence length  $L_c$  equal to the confocal parameter of the focus.<sup>5,6</sup> For Xe in this region of the spectrum this will require an atom density between  $10^{15}$  and  $10^{16}$  atoms/cm<sup>3</sup>, and thus Xe pressures in the range of 0.1 Torr. At this pressure, and for a pulse length of 30 psec, avalanche breakdown would require a power density of about  $5 \times 10^{15}$  W/cm<sup>2</sup><sup>11</sup>; the assumption of multiphoton breakdown is thus well satisfied.

In recent weeks the processes  $3 \times 5320 \text{ \AA} \rightarrow 1773 \text{ \AA}$  and  $5 \times 5320 \text{ \AA} \rightarrow 1064 \text{ \AA}$  have been demonstrated experimentally. Conversion efficiencies are comparable and measurements will be reported subsequently.<sup>3</sup>

The final three examples in Table I are 5th-, 7th-, and 15th-order processes in singly ionized Li to generate radiation at 236 Å, 169 Å, and 177 Å. Ionization will be accomplished by the incident laser pulse. At ion densities of  $\sim 10^{16}$  ions/cm<sup>3</sup>, recombination times are several nanoseconds,<sup>12</sup> and each atom need be ionized only once during the incident laser pulse. Because of the tight focus, this will require only about  $10^{-8}$  of the incident pulse energy.

Even at its lower efficiency, the process  $15$

$\times 2660 \text{ \AA} \rightarrow 177.3 \text{ \AA}$  may be an attractive early source of coherent soft-x-ray radiation. It makes use of a fortuitous coincidence with the  $1s^2[{}^1S]0-3p[{}^1P^o]1$  transition of Li<sup>+</sup> at 178.015 Å<sup>10</sup> (2160 cm<sup>-1</sup> below the generated frequency). As a result of longer coherence lengths in this region of the spectrum, it is almost essential that coincidences of this type be utilized. Assuming an incident peak power of  $10^{10}$  W, to attain the limiting power density, the laser must be focused to a confocal parameter = 0.43 cm. For  $L_c$  = confocal parameter, at an oscillator strength of 0.07 (equal to that of the comparable  $1s-3p$  transition in He), this requires an ion density of  $1.5 \times 10^{18}$  ions/cm<sup>3</sup>. At this high density the condition on inverse bremsstrahlung ionization<sup>11</sup> is close to being violated.

By using sum-frequency processes, one photon of a tunable dye laser might be utilized to allow close frequency coincidences and thus to reduce the required ion or atom density. Sum-frequency processes might also be used to inject high-power, lower-frequency radiation and thus to reduce the required power density at the highest applied frequency. Phase-matching techniques<sup>2,6</sup> may also be used to increase the conversion efficiencies of Table I.

The author gratefully acknowledges helpful and interesting discussions with H. Rebb, D. M. Bloom, G. C. Bjorklund, A. Gold, A. H. Kung, A. E. Siegman, E. A. Stappaerts, and J. F. Young.

\*Work supported by the U. S. Office of Naval Research, the U. S. Air Force Cambridge Research Laboratories, and the U. S. Army Research Office.

<sup>1</sup>G. S. Voronov and N. B. DeLone, Zh. Eksp. Teor. Fiz. Pis'ma Red. **1**, 42 (1965) [JETP Lett. **1**, 66 (1965)].

<sup>2</sup>A. H. Kung, J. F. Young, and S. E. Harris, Appl.



- Phys. Lett. 22, 301 (1973).
- <sup>3</sup>A. H. Kung, E. A. Stappaerts, J. F. Young, and S. E. Harris, to be published.
- <sup>4</sup>J. A. Armstrong, N. Bloembergen, J. Ducuing, and P. S. Pershan, Phys. Rev. 127, 1918 (1962).
- <sup>5</sup>J. F. Ward and G. H. C. New, Phys. Rev. 185, 57 (1969).
- <sup>6</sup>R. B. Miles and S. E. Harris, IEEE J. Quantum Electron. 9, 470 (1973).
- <sup>7</sup>H. B. Bebb and A. Gold, Phys. Rev. 143, 1 (1966).
- <sup>8</sup>V. M. Morton, Proc. Phys. Soc., London 92, 301 (1967).
- <sup>9</sup>L. V. Keldysh, Zh. Eksp. Teor. Fiz. 47, 1945 (1964) [Sov. Phys. JETP 20, 1307 (1965)].
- <sup>10</sup>C. E. Moore, *Atomic Energy Levels*, U. S. National Bureau of Standards, National Standard Reference Data Systems-35 (U. S. GPO, Washington, D. C., 1971), Vols. 1 and 3.
- <sup>11</sup>M. Young and M. Hercher, J. Appl. Phys. 38, 4393 (1967); A. V. Phelps, in *Physics of Quantum Electronics*, edited by P. L. Kelley et al. (McGraw-Hill, New York, 1966).
- <sup>12</sup>H. R. Griem, *Plasma Spectroscopy* (McGraw-Hill, New York, 1964).

MICROWAVE LABORATORY

2178

STANFORD UNIVERSITY